
TOWARDS ENERGYGPT: A LARGE LANGUAGE MODEL SPECIALIZED FOR THE ENERGY SECTOR

Amal Chebbi, Ph.D.

Data Scientist
Fitila Labs
Chicago, IL

amal.chebbi@fitila.ai

Babajide Kolade, Ph.D., PE.

Founder and Technical Director
Fitila Labs
Chicago, IL

babajide.kolade@fitila.ai

ABSTRACT

Large Language Models have demonstrated impressive capabilities across various domains. However, their general-purpose nature often limits their effectiveness in specialized fields such as energy, where deep technical expertise and precise domain knowledge are essential. In this paper, we introduce EnergyGPT, a domain-specialized language model tailored for the energy sector, developed by fine-tuning LLaMA 3.1-8B model using Supervised Fine-Tuning on a high-quality, curated corpus of energy-related texts. We present a complete development pipeline, including data collection and curation, model fine-tuning, benchmark design and LLM-judge choice, evaluation and deployment. Through this work, we demonstrate that our training strategy enables improvements in domain relevance and performance without the need for large-scale infrastructure. By evaluating the performance of the model using domain-specific question-answering benchmarks, our results demonstrate that EnergyGPT outperforms the base model in most of the energy-related language understanding and generation tasks.

Keywords Large Language Models · Domain Adaptation · Supervised Fine-Tuning · Energy · Data Curation · EnergyGPT · Deployment

1 Introduction

The rapid progress in natural language processing (NLP), fueled by the development of pre-trained large language models (LLMs), has revolutionized various applications across industries. These models, trained on vast general-purpose datasets, exhibit exceptional capabilities in text generation, question answering, and reasoning. However, their general-purpose nature might limit their effectiveness in specialized fields such as energy, where technical accuracy, deep domain knowledge, and contextual understanding are essential. The energy sector encompasses diverse disciplines, including power systems, renewable energy, oil and gas, energy policy, and engineering research, etc., each requiring precise, industry-specific expertise that general LLMs might not capture effectively. While models such as OpenAI's GPT, Meta Platform's LLaMA, and DeepSeek have demonstrated impressive capabilities in general NLP tasks, their general-purpose nature presents several key challenges:

- **Technical Precision and Domain Knowledge:** General LLMs often generate factually incorrect or overly generalized responses due to their lack of deep expertise in energy-related subjects.
- **Contextual Relevance:** Many energy-sector queries involve technical language, regulatory standards, and industry-specific frameworks, which general models may misinterpret or oversimplify.
- **Data Limitations:** Pretrained models are primarily trained on open web data, books, and general corpora, which contain limited energy-sector data, leading to knowledge gaps.
- **Lack of Adaptation to Industry Needs:** Energy professionals require AI models that can assist in research, decision-making, and predictive analysis, which demands a higher degree of specialization than general LLMs can provide.

To address these challenges, we introduce EnergyGPT, a specialized language model tailored for the energy sector. Instead of training of a language model from blank slate or applying Continual Pretraining (CP), which are computationally expensive and data-intensive, we strategically employ Supervised Fine-Tuning (SFT) to adapt a pre-trained LLM using a carefully curated corpus of energy-related data. This approach enables the model to internalize domain-specific knowledge while maintaining its general capabilities, significantly improving its performance on energy-related queries. A similar adaptation strategy, based on LoRA, has been explored in prior work [1].

Key Contributions This paper presents a systematic framework for developing EnergyGPT, with the following key contributions:

- **Energy-Sector Dataset Curation:** We present a method for curating domain-specific training corpus from open literature. Here, we construct a high-quality corpus of energy-related literature, including peer-reviewed research papers and other text extracted from public resources. The dataset undergoes rigorous preprocessing, including quality filtering, deduplication, and semantic selection, to ensure relevance and consistency.
- **Data Structuring for Context-Aware Learning:** To improve logical consistency and knowledge retention, we structure our dataset into input-output pairs (e.g. $P_1 : C_1C_2 \ C_3C_4$, $P_2 : C_2C_3 \ C_4C_5$), enabling coherent text generation.
- **Efficient Model Adaptation through SFT:** We apply Supervised Fine-Tuning on LLaMA 3.1-8B [2], leveraging its strong foundational capabilities while adapting it for energy-sector applications.
- **Comprehensive Evaluation and Benchmarking:** We assess EnergyGPT using domain-specific question-answering benchmarks, demonstrating performance improvements in technical accuracy, contextual relevance, and response quality over the baseline LLM.
- **Scalable Framework for Adapting LLMs:** We propose a scalable and cost-efficient pipeline for adapting general LLMs to specialized fields using SFT. Our method can be extended beyond energy to create highly specialized AI assistants for other technical domains.
- **LLM Model Deployment:** We deploy EnergyGPT using a production-grade NIM server, first hosted on-premises for local testing and subsequently deployed in Azure. We integrate Azure API Management (APIM) to provide a secure, scalable REST API and monitor usage.

The remainder of this paper is organized as follows: Section 2 reviews related work on domain-specific LLMs and Supervised Fine-Tuning methods. Section 3 details the data collection, preprocessing, and structuring techniques used to curate a high-quality energy-related dataset. Section 4 describes the model adaptation strategy, including the SFT process, training setup, and hyperparameter optimization. Section 5 introduces a custom benchmark developed to evaluate EnergyGPT as well as the methodology for selecting an LLM-judge. Section 6 presents the experimental results, evaluating EnergyGPT’s performance along with comparisons to the baseline model. Section 7 details the deployment setup, explaining how EnergyGPT is served via a production-grade NIM server, first on-premises for local testing and subsequently in Azure integrated with Azure API Management for secure and scalable access. Section 8 discusses key challenges, limitations, and potential enhancements for EnergyGPT, as well as future research directions. Finally, Section 9 summarizes the key findings and broader implications of this work.

2 Related Work

Large language models have achieved remarkable success in various domains, demonstrating strong capabilities in text generation, question answering, and reasoning. However, many specialized domains such as healthcare [3], finance [4], climate [5], legal and technology possess unique linguistic nuances, technical terminologies, and contextual dependencies that general-purpose LLMs fail to capture effectively [6]. This disparity between the broad linguistic knowledge encoded in pre-trained models and the specialized knowledge requirements of specific fields highlights the need for adapting LLMs to domain-specific applications.

Domain-Specific Adaptation in Language Models

In NLP literature, two primary strategies have emerged for developing domain-specific language models: **training a foundation model from scratch** and **continual pretraining** on domain-specific corpora. Many research efforts have focused on building domain-specialized language models from the ground up, leveraging industry-specific knowledge to enhance their capabilities in targeted applications. For instance, BloombergGPT [4] was trained on an extensive corpus of financial texts, improving performance in economic forecasting, market analysis, and financial sentiment detection. Similarly, in the biomedical field, BioGPT [7] was developed using biomedical

literature, enabling enhanced capabilities in biomedical text generation and mining. Likewise, BioMedLM [8], trained on PubMed and other medical literature, was designed to advance medical language understanding and question answering. Meanwhile, Galactica [9] was developed to store, integrate, and reason over scientific knowledge, making it particularly valuable for researchers and scientists working in interdisciplinary fields.

Training a foundation model from scratch requires learning from more than 100 billion tokens [10, 4, 9] of raw domain-specific data, necessitating the meticulous curation of large-scale domain datasets. These models undergo self-supervised learning on unlabeled text [11], leveraging techniques such as next-token prediction [12] and masked language modeling [13], where the model sequentially predicts words while reconstructing masked tokens. While this approach maximizes domain adaptation, it is highly resource-intensive, demanding substantial computational power, large-scale datasets, and extensive infrastructure [14]. Consequently, despite its advantages, training domain-specific models from scratch remains impractical for many specialized fields due to the immense costs and data requirements [15].

An alternative approach to training domain-specific models from scratch is domain-adaptive continual pretraining (DACP) [16], also known as continual pretraining (CP). This method involves further pretraining an existing foundation model on additional domain-specific unlabeled datasets [16, 17, 18] using self-supervised learning techniques. By extending the pretraining phase of a general-purpose LLM, such as GPT, LLaMA, or other transformer-based models, on a curated domain-specific corpus, the model gradually adapts to specialized terminologies, contextual nuances, and industry-specific patterns while retaining its foundational linguistic knowledge. Domain-adaptive pretraining offers a computational advantage over training a model from scratch, as it leverages an already well-trained base model, reducing the need for massive datasets and extensive compute resources while still achieving significant domain adaptation. Studies have shown that this method significantly improves performance on specialized domains without requiring complete retraining [17, 19, 20] and also facilitates the continuous integration of emerging domain knowledge as new data becomes available [21, 22, 23].

2.1 SFT for Domain Adaptation of LLMs

Supervised Fine-Tuning (SFT) has emerged as a practical and resource-efficient approach to adapt large language models for use in specialized domains. Unlike pretraining, which requires massive amounts of unlabeled data and extensive compute power, SFT focuses on refining a pretrained model using a smaller, carefully curated dataset of high-quality input-output pairs. These pairs are crafted to reflect the specific language, concepts, and reasoning patterns of a target field, allowing the model to better align with domain-specific tasks and knowledge requirements [24].

SFT typically begins by initializing from a general-purpose or continually pretrained checkpoint. The model is then fine-tuned using supervised examples tailored to the domain. These examples may include question-answer pairs, document summaries, or instruction-style prompts, each chosen based on the nature of the downstream application [25]. By exposing the model to structured, domain-relevant supervision, SFT enhances the model's ability to understand and generate content that is accurate, coherent, and task-aligned.

One of the key advantages of SFT is its efficiency with data. Because it builds on top of existing pretrained models, the amount of labeled data required for meaningful adaptation is relatively modest than what is needed for pretraining. This is particularly valuable in fields where labeled data is limited or expensive to obtain, especially when expert annotation is needed. SFT also supports an iterative refinement process: the model can be updated over time as new data becomes available or as task requirements evolve, without needing to restart the training pipeline from scratch. In practice, SFT has been shown to improve factual reliability, reduce hallucinations, and offer greater control over model outputs [26].

2.2 Other Cost Efficient Methods for Domain Adaptation of LLMs

In recent years, several alternative strategies for domain adaptation have emerged as cost-efficient, scalable, and performance-preserving solutions to the challenges of full fine-tuning using SFT. Parameter Efficient Fine-Tuning (PEFT) techniques such as Low-Rank Adaptation (LoRA) [27], Quantized LoRA (QLoRA) [28], and adapter-based methods [29] modify pre-trained models by introducing lightweight, trainable components. These methods substantially reduce computational and memory requirements, making them well-suited for use in resource-constrained environments without significantly compromising performance for specific tasks or domains.

However, with these reduced computational footprint advantage come notable limitations that may restrict the effectiveness of those methods in fully specializing LLMs. For example, instead of updating all the weights of the

pre-trained model, LoRA and QLoRA inject low-rank trainable matrices into specific layers, and only these additional parameters are optimized during fine-tuning, leaving the original model weights frozen [27].

Adapter-based methods follow a similar philosophy, inserting small bottleneck modules (e.g., feed-forward neural networks) between transformer layers to enable task-specific learning with minimal parameter updates. While this dramatically improve efficiency, these methods may fall short in capturing complex domain-specific representations, particularly in tasks requiring deep semantic understanding or multi-step reasoning. The frozen nature of the base model can become a bottleneck when substantial adaptation is needed. Furthermore, in the case of QLoRA, the use of aggressive quantization, typically to 4-bit precision, enhances memory savings but can also introduce numerical instability, potentially degrading performance on tasks sensitive to precision, such as arithmetic or structured reasoning [30].

2.3 Other Strategies for Knowledge-Intensive NLP

Similarly, Retrieval-Augmented Generation (RAG) [31], which augments models with external knowledge at inference time, relies heavily on the quality and relevance of the retrieval corpus. Its performance is highly sensitive to retrieval parameters such as the number of retrieved chunks and the accuracy of the ranking algorithm, poor retrieval can introduce irrelevant or conflicting context [32]. Moreover, external lookups at inference time adds infrastructure complexity, inference latency, and increased vulnerability to retrieval noise, especially in dynamic or low-resource domains [33].

3 Data Preparation: Methodology

A critical step in developing a domain-specific LLM is the curation of a high-quality, domain-focused dataset. This section presents the methodology used to develop an energy-specific dataset for training EnergyGPT, including data collection, curation, preprocessing, and the strategy for generating input-output pairs.

3.1 Data Collection

Our training corpus is constructed by combining publicly available energy-related literature, including scientific research papers from ASME and other reputable sources, along with a filtered subset of The Pile dataset [34] that is relevant to the energy sector. The Pile is a diverse English text corpus sourced from 22 high-quality domains, spanning academic, technical, legal, and online communities.

ASME journals subset. We assembled an ASME-specific corpus from the authors' licensed collection, accrued over two decades, using a two-stage screening based on topical fit and influence. We prioritized flagship titles central to EnergyGPT's scope, e.g., the *ASME Journal of Heat and Mass Transfer*, the *Journal of Mechanical Design*, and the *Journal of Energy Resources Technology*. Journal prioritization combined topical fit (per publisher scope statements) with publicly available influence indicators (e.g., SJR/JCR), rather than convenience sampling. Only content permissible for text-and-data mining was processed. No full-text redistribution occurs; we retain cleaned text and derived statistics for internal modeling. The resulting ASME subset comprises approximately 40k articles spanning roughly two decades and yields on the order of 1.8B tokens after cleaning and normalization.

3.2 Data Cleaning: Energy-related Scientific Literature

For the scientific literature, we extracted textual data and mathematical equations from 40k+ scientific papers spanning various energy-related disciplines. To ensure data quality and consistency, the collected corpus underwent a rigorous preprocessing pipeline. First, extraneous metadata, such as publisher and submission details, DOI links, acknowledgments, etc., was removed to eliminate non-essential content. Additionally, inline citations and reference markers were cleaned to prevent citation numbers and bibliography links from interfering with text readability and coherence. Given that the dataset contained documents in multiple formats and encoding schemes, Unicode normalization was applied to standardize character encoding, while OCR artifacts were corrected to improve text integrity. Furthermore, a portion of the dataset contained broken LaTeX formatting in mathematical expressions, which was systematically corrected to preserve the structural integrity of equations.

These preprocessing steps were crucial in creating a clean, structured, and high-quality dataset for training EnergyGPT, ensuring that the model learns from accurate, domain-specific content without unnecessary noise or inconsistencies.

3.3 Data Curation: The Pile

The following subsections describe the methodology used to extract relevant subsets from The Pile for training EnergyGPT. For this step, we used **NVIDIA NeMo Curator** [35], which is an open-source data processing tool designed for large-scale corpus filtering and transformation provided by NVIDIA. This process involves applying rigorous quality filtering, deduplications and identifying energy-related documents from The Pile.

3.3.1 Quality Filtering

A significant portion of raw text scraped from the internet is unsuitable for training language models, as it often contains broken HTML, non-printable characters, or incoherent and low-quality content. Training on such noisy data can negatively impact the model’s overall performance and output quality. In the development of GPT-3 [36], for example, this issue was mitigated through a quality filtering step applied to the dataset. The developers trained a logistic regression classifier to distinguish high-quality text from gibberish using low-dimensional document representations [37]. Following this approach, [1] trained a similar logistic regression model using 150k+ samples extracted from Project Gutenberg [38] as positive high-quality examples and 200k+ randomly sampled documents from the unfiltered Common Crawl for negative examples. In our work, we used a similar quality classifier, Quality Classifier DeBERTa [39, 40], that is trained to categorize documents into high, medium, or low quality based on their textual coherence and structure. Only documents labeled as high or medium quality were retained for the next stage of processing.

3.3.2 Exact De-duplication

Large-scale text corpora sourced from the web are known to contain a substantial amount of duplicated content. These duplicates often stem from repeated web pages, mirrored sites, or boilerplate text structures. For instance, [41] reports that 12% of Common Crawl snapshots are composed of duplicate documents, with a significant portion, up to 40%, being exact duplicates. Training large language models on such highly redundant datasets across multiple epochs can be suboptimal, leading to inefficiencies in both computational resource usage and generalization performance [42, 43]. To mitigate these issues, deduplication is a critical preprocessing step. Prior work such as [44] proposed efficient algorithms for detecting exact duplicates based on suffix tree representations, which enable the identification of repeated substrings in linear time. While effective, such methods may introduce substantial computational overhead when applied to extremely large datasets (e.g. the Pile).

In our preprocessing pipeline, we adopt a more scalable and computationally lightweight approach based on hashing techniques. Each document is processed to generate a unique hash signature, and only one instance is retained per unique hash, ensuring that exact duplicates are efficiently removed from the corpus before further processing [45].

3.3.3 Fuzzy De-duplication

While exact deduplication effectively removes identical documents, it fails to capture near-duplicate documents that share significant textual overlap but are not byte-for-byte identical. Such near-duplicates often result from minor edits, formatting differences, or slight paraphrasing [46]. To address this limitation, we employed fuzzy deduplication techniques [45] to detect and eliminate near-duplicate documents, which are particularly prevalent in large-scale corpora like The Pile.

To identify near-duplicate documents in our dataset, we began by vectorizing each document using a hashing-based method, followed by computing MinHash signatures [47, 48] to compactly represent their content. These signatures allowed us to efficiently estimate Jaccard similarity without the need for exhaustive pairwise comparisons. We then applied Locality-Sensitive Hashing (LSH) on the MinHash representations [48] to group potentially similar documents into candidate buckets. Our goal with LSH was to ensure that documents with high similarity would likely be grouped into the same bucket (Appendix A.1). To achieve this, we configured LSH with 20 bands of 13 hash values each, resulting in a total of 260 hash functions per document.

Once candidate buckets were formed, we refined them to eliminate false positives introduced during the hashing step. For each bucket, we randomly selected around 10% anchor documents, compared each sampled document d_i to the remaining documents using Jaccard similarity and only documents with similarity score exceeding $\tau = 0.8$ were marked as duplicates and linked to their corresponding anchors. After processing all buckets, we built a sparse graph where nodes represented documents and edges connected documents identified as near-duplicates. Finally, we extracted connected components from the graph, with each component representing a group of near-duplicates and from each group, we retained a single representative document to construct the final deduplicated dataset. These steps were carried out using NVIDIA NeMo Curator [45], below in 1 is a comprehensive representation of the fuzzy deduplication workflow.

Algorithm 1 Fuzzy Deduplication Pipeline

- 1: **Input:** Dataset $\mathcal{D} = \{d_1, d_2, \dots, d_n\}$, Jaccard similarity threshold $\tau = 0.8$
- 2: **Output:** Deduplicated dataset \mathcal{D}'
- 3: **MinHash Signature Generation**
- 4: **for** each document $d_i \in \mathcal{D}$ **do**
- 5: Compute MinHash signature h_i for d_i .
- 6: **end for**
- 7: **Locality-Sensitive Hashing (LSH)**
- 8: Partition $\{h_i\}$ into 20 bands \times 13 hashes per band $\Rightarrow 260$ hash functions.
- 9: Group documents into candidate buckets based on matching LSH bands.
- 10: **Candidate Bucket Refinement**
- 11: **for** each candidate bucket B **do**
- 12: Randomly select anchor documents from B .
- 13: **for** each anchor document $d_a \in B$ **do**
- 14: **for** each remaining document $d_j \in B$ **do**
- 15: Compute $J(d_a, d_j)$ using MinHash.
- 16: **if** $J(d_a, d_j) \geq \tau$ **then**
- 17: Mark d_j as a near-duplicate and link it to d_a .
- 18: **end if**
- 19: **end for**
- 20: **end for**
- 21: **end for**
- 22: **Graph-Based Deduplication**
- 23: Construct a sparse graph $G = (V, E)$ where:
 - V = set of documents.
 - E = edges between documents with $J(d_i, d_j) \geq \tau$.
- 24: Extract connected components $\{C_1, C_2, \dots\}$ from G .
- 25: Retain one representative document per component.
- 26: **Final Dataset Construction**
- 27: Combine all representative documents to produce \mathcal{D}' .
- 28: **return** \mathcal{D}'

3.3.4 Semantic Filtering

Since our source corpora contain a broad mix of content spanning numerous domains, performing semantic filtering is essential to isolate energy-related data [49]. To achieve this, we constructed a set of expertly curated reference queries representing various topics within the energy domain (see Appendix. B). We then leveraged transformer-based embedding models from the Sentence Transformers library [50] to encode both the reference queries and candidate documents. Specifically, we experimented with several state-of-the-art models, including `intfloat/e5-large-v2` [51], `BAAI/bge-base-en-v1.5` [52], and `sentence-transformers/all-mpnet-base-v2` [53], to evaluate their effectiveness in capturing semantic similarity. To scale processing across large datasets efficiently, we implemented a multi-GPU filtering pipeline. Each GPU was assigned a subset of the input shards and independently computed normalized embeddings for all documents. For each document embedding, we calculated the cosine similarity against all reference query embeddings and retained only documents with a similarity score above a threshold of 0.8.

3.4 Data Balancing

The final corpus used to train EnergyGPT was constructed by mixing two primary sources to create an energy-specialized dataset: (1) energy-related text extracted from scientific papers published in reputable journals, and (2) a filtered, semantically relevant subset of The Pile dataset. This mixture ensures a balance between highly specialized technical content and broader contextual information within the energy domain. Following best practices recommended in [54, 55], we included a small proportion of randomly selected, high-quality general-domain content from

The Pile. This deliberate injection of general data, approximately 1.4% of the total corpus, helps preserve the model’s general language capabilities and mitigate catastrophic forgetting. The data preparation process is illustrated in Figure 1.

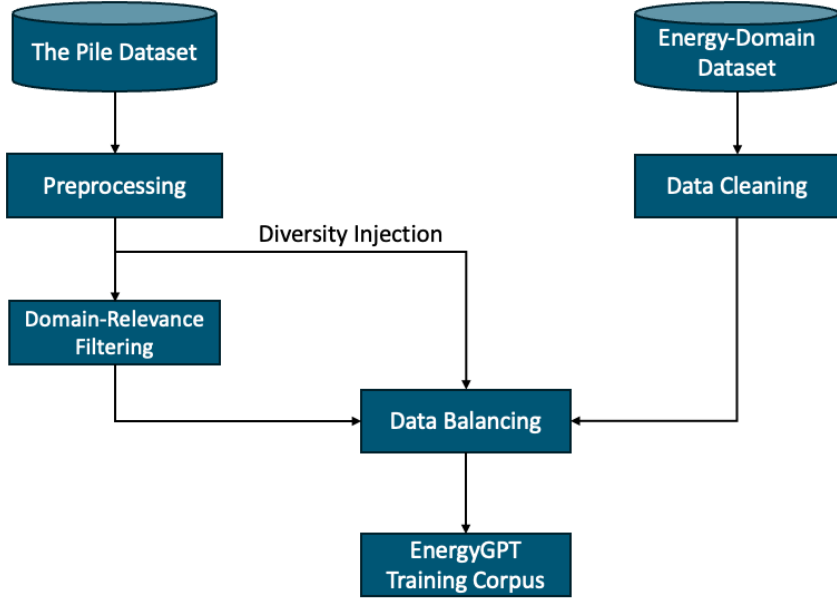


Figure 1: Data preparation pipeline for fine-tuning EnergyGPT.

The table 1 below summarizes the composition of the final dataset used for fine-tuning EnergyGPT.

Dataset	Quantity (tokens)	Weight in training mix
Scientific Papers	~1.8 billion	82.9%
The Pile (relevant)	~0.34 billion	15.7%
The Pile (filtered)	30 Million	1.4%

Table 1: Datasets used for fine-tuning EnergyGPT. Weight in training mix refers to the fraction of examples during training that are drawn from a given dataset.

3.5 Data Pairs Generation for SFT

Fine-tuning a large language model using supervised fine-tuning requires the training data to be organized into input-output pairs. To support this, we developed an efficient pipeline that transforms each document into structured data pairs. For data extracted from The Pile dataset, each document was first split into sentence-aware and equation-aware chunks, ensuring that sentence boundaries were preserved and that mathematical equations remained intact and not broken apart (i.e., not fragmented across chunks). We limited each chunk to around 600 tokens to stay within the model’s capacity and to keep the content manageable, we have used LLaMA 3.1-8B tokenizer throughout this process. From the resulting chunks, we generated overlapping input-output pairs with a stride of C_{n+2} , allowing contextual information to flow smoothly across sequences. This approach helped maintain consistency in structure and token length across pairs. The pairing strategy we followed is illustrated below:

$$\begin{aligned}
 \text{Pair 1: } & \text{Input } (C_1 \ C_2 \ C_3) \longmapsto \text{Output } (C_4 \ C_5 \ C_6) \\
 \text{Pair 2: } & \text{Input } (C_3 \ C_4 \ C_5) \longmapsto \text{Output } (C_6 \ C_7 \ C_8)
 \end{aligned}$$

where C_i denotes the i^{th} chunk extracted from a document d .

For data extracted from the scientific literature, each document is first segmented into paragraph-aware, sentence-aware, and equations-aware chunks. These segments are then organized into input-output pairs using a sliding window

strategy with a stride of one paragraph. Each pair is constrained to a maximum of 4,096 tokens, with an effort made to balance input and output lengths, typically targeting around 2,000 tokens per side, to prevent the model from overfitting on short output. Thus the number of chunks included in the input and output is variable, depending on their token lengths of paragraphs. An example of the pairing strategy is illustrated below:

$$\begin{aligned} \textbf{Pair 1:} \quad & \text{Input } (P_1 \ P_2 \ P_3) \longmapsto \text{Output } (P_4 \ P_5) \\ \textbf{Pair 2:} \quad & \text{Input } (P_3 \ P_4) \longmapsto \text{Output } (P_5 \ P_6 \ P_7) \end{aligned}$$

where P_i denotes the i^{th} paragraph extracted from a document d .

The total number of pairs generated and their sources are summarized in Table 2.

Dataset	Number of pairs
Scientific Papers	517,716 pairs
The Pile (relevant)	193,448 pairs
The Pile (filtered)	20,781 pairs

Table 2: Data pairs used for fine-tuning EnergyGPT.

4 EnergyGPT Training Approach

This section describes the overall training strategy, infrastructure, and experimental setup used to develop EnergyGPT. More Details and explanations can be found in Appendix C.

4.1 Base Model

In our work, we adopted the open-source LLaMA 3.1-8B as the foundation model of EnergyGPT. The architectural specifications of LLaMA 3.1-8B are presented in Table 3.

Parameter	Configuration
Hidden size	4096
Heads	32
Layers	32
Vocab size	128,256
Sequence length	131,072

Table 3: LLaMA 3.1-8B Model Architecture Settings.

4.2 Training Configuration and Hardware

For the fine-tuning of EnergyGPT, we leveraged NVIDIA’s high-performance hardware and software stack. The training was conducted on a compute cluster equipped with 4 NVIDIA A100 GPUs (80GB each), using the **NVIDIA NeMo** framework and **Megatron-LM** toolkit [56, 57]. The process involved 2 full passes (epochs) over the curated dataset. To maximize resources utilization while avoiding out-of-memory errors, we employed intra-layer model parallelism, which distributes matrix operations within each transformer layer across multiple GPUs [46]. Throughout training, we regularly monitored progress and evaluated performance by calculating the validation loss (see Appendix C). The 10 best-performing checkpoints were saved at the end for subsequent use. A detailed summary of the training configuration and hyperparameters is provided in Table 4.

Hyper-Parameter	Configuration
Base model	LLaMA 3.1-8B
Compute infrastructure	4 GE A100-80GB GPUs
Training duration	≈ 6 days
Epochs	2
Global batch size	256
Micro batch size	8
Max sequence length	8192
Max learning rate	2e-5
Optimizer	Distributed Fused Adam
Adam beta weights	[0.9, 0.95]
Learning rate scheduler	Cosine Annealing
Weight decay	0.01
Warm-up steps	280
Gradient clipping	1.0

Table 4: Hyperparameters for fine-tuning EnergyGPT.

5 EnergyGPT Benchmark

This section introduces the composition of the benchmark used to evaluate EnergyGPT, along with the methodology for selecting a high-quality LLM to serve as an automated judge for grading and evaluation of the models responses.

5.1 Benchmark Design

We developed a specialized benchmark for evaluating EnergyGPT, consisting of 463 question-answer pairs designed to assess the model’s performance across a range of cognitive tasks related to energy science. The benchmark includes multiple-choice, true/false, factual, and open-ended questions categorized by difficulty levels: easy, medium, hard, and challenging. These questions are divided into three main sets, each serving a distinct purpose: (1) 100 true/false statements focused on evaluating the model’s grasp of fundamental energy concepts and its ability to handle binary factual reasoning; (2) 233 multiple-choice questions aimed at testing the model’s capability to recognize correct information among distractors and to perform basic reasoning under constrained options; (3) 130 open-ended energy-related questions that vary in difficulty and include factual recall, designed to assess the model’s depth of understanding, ability to generate informative-coherent answers, and performance on complex, open-form queries. To illustrate the structure and content of the benchmark, a sample of questions are provided in the supplementary text boxes in Appendix D.

In our benchmarking strategy, we evaluated the model’s ability to select the correct answer by employing a structured prompting approach, which constrained the model’s response to a single word or letter, ideal for multiple-choice or binary (True/False) questions. Two distinct prompt templates were used to instruct the model:

1. Prompt for Multiple-choice questions:

You are an expert in the energy field answering multiple-choice questions. Please provide only the correct answer key for the following question; you do not need to include an explanation. {q}

followed by:

Answer Now:

2. Prompt for True/False statements:

Determine whether the following statement is true or false. Respond with either "True" or "False" only, no explanation needed.
Statement: {q}

followed by:

Answer:

The benchmarking was conducted with a deterministic setup without sampling (that is, $T = 0$) to ensure consistency in responses.

5.2 Choice of LLM Judge

Evaluating the quality of generated responses in specialized domains like energy is both essential and resource-intensive. Human expert evaluation remains the gold standard but is time-consuming, costly, and difficult to scale across large datasets. As the diversity and volume of generated outputs increase, there is a growing need for automated, scalable, and reliable evaluation frameworks that still approximate human judgment. In this context, LLM-as-a-judge, the use of a strong language model to evaluate the output of another, offers a compelling alternative. Recent work [58, 59] has shown that well-aligned LLMs, such as GPT-4, can reach over 80% agreement with human annotators, making them viable surrogates for high-quality evaluation. However, this alignment is not guaranteed across all models, tasks, or domains. Thus, choosing an appropriate judge LLM is critical to ensure the integrity and reliability of automated evaluation pipelines.

Experimental Setup

To identify a judge model that closely mirrors human expert preferences in the energy and technical QA domain, we evaluated several state-of-the-art LLMs. We used responses generated by LLaMA 3.1-8B for 20 energy-related queries. Each response was scored along seven evaluation criteria: Relevance, Correctness, Technical Level, Scientific Level, Explainability, Conciseness and Coherence. Each LLM judge was instructed to act as a domain expert and return a structured JSON containing integer scores (0-10) for each dimension. For ground truth, expert human annotator independently scored the same set of responses using identical criteria.

Results and Analysis

Figure 2 presents a radar plot comparing the average scores assigned by each LLM judge model against human annotations (black dashed line) across seven evaluation criteria: relevance, correctness, technical level, scientific level, explainability, conciseness, and coherence. The evaluated models include GPT-4, GPT-4o, GPT-4.1, several Claude variants (Haiku, Sonnet), Gemini models, and LLaMA 3.3-70B. Human annotators consistently assigned more conservative scores, particularly in correctness and technical rigor, revealing a calibration gap in many LLM judges. Among all candidates, the Claude Sonnet-4 model most closely mirrored the human annotator scoring profile across all dimensions. Notably, it exhibited accurate calibration on technical depth and correctness, strong alignment in explainability and coherence, and minimal deviation in conciseness and relevance. In contrast, while other models performed well in aggregate, many showed a tendency to systematically overestimate performance, given our objective of selecting an automated judge that faithfully approximates expert human evaluation, we designate Claude Sonnet-4 as the LLM judge for this study.

6 Results and Achievements

To illustrate how the language model’s performance evolved during fine-tuning, we present the validation loss curve in Figure 3. Validation loss was computed at regular intervals, every 200 training steps, using a held-out validation set comprising 2% of the dataset (approximately 15,000 input-output pairs). The plot shows the cross-entropy validation loss as a function of consumed steps. A slight increase in loss is observed at the beginning, likely due to initial optimization dynamics, followed by a steady decline. Training was stopped early, after observing that the validation loss plateaued for three consecutive evaluations and subsequently began to increase while the training loss continued to decrease. The full fine-tuning process spanned 3,040 steps and was completed in approximately 6 days. This drop in cross-entropy translates into a reduction in perplexity roughly by 5%.

For the open-ended question benchmark, we conducted an automated assessment using the LLM-judge (see 5.2). The evaluation compared responses generated at deterministic settings (temperature T set to 0) by the foundation model LLaMA 3.1-8B and EnergyGPT. The LLM judge was instructed to score each response on a scale from 0 to 10, based on multiple criteria including relevance, coherence, technical depth, consistency, and diversity. For the reliability of the automated evaluations, a human evaluator randomly inspected a subset of the generated answers and confirmed the consistency and accuracy of the LLM-judges scoring.

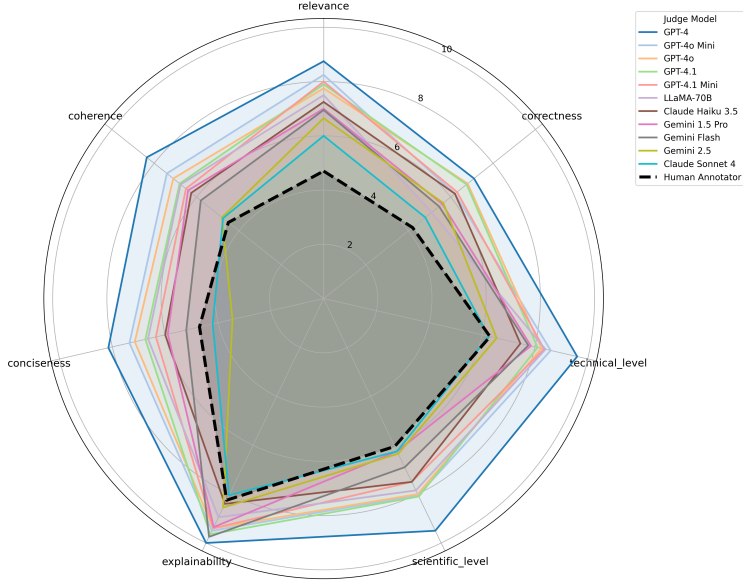


Figure 2: Radar plot comparing average evaluation scores assigned by various LLM judge models and a human annotator across seven criteria: relevance, correctness, technical level, scientific level, explainability, conciseness, and coherence.

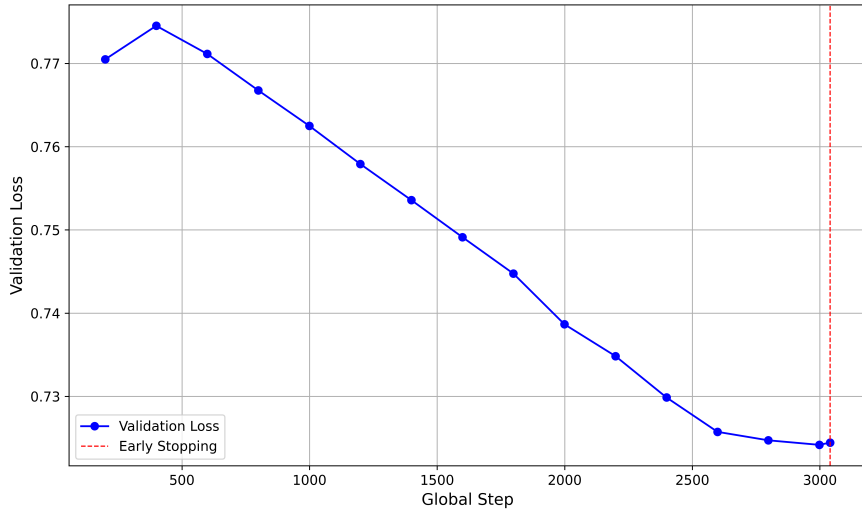


Figure 3: Cross-entropy validation loss vs. consumed steps.

Evaluations from both the human annotator and an LLM judge indicate that EnergyGPT consistently outperforms the foundation model across multiple dimensions, notably technical depth, coherence, and relevance. EnergyGPT generates responses that are more detailed, contextually appropriate, and semantically rich. In contrast, the foundation model frequently deviates from the topic or fails to maintain focus. Samples of generated responses on multiple queries by both models are presented in Appendix E.1. Presented in Figure 4, the radar plot illustrates the comparative performance of EnergyGPT and LLaMA 3.1-8B across seven evaluation dimensions: relevance, correctness, technical level, scientific level, explainability, conciseness, and coherence.

For multiple choice and true/false questions, both models performed well overall (see Table 5). However, EnergyGPT consistently adhered to the prompt instructions by providing direct answers. Most of its responses began with the correct option or a clear "True" or "False" designation, occasionally followed by brief explanations. In contrast, the base model often included lengthy or unnecessary explanations and frequently failed to clearly indicate the correct

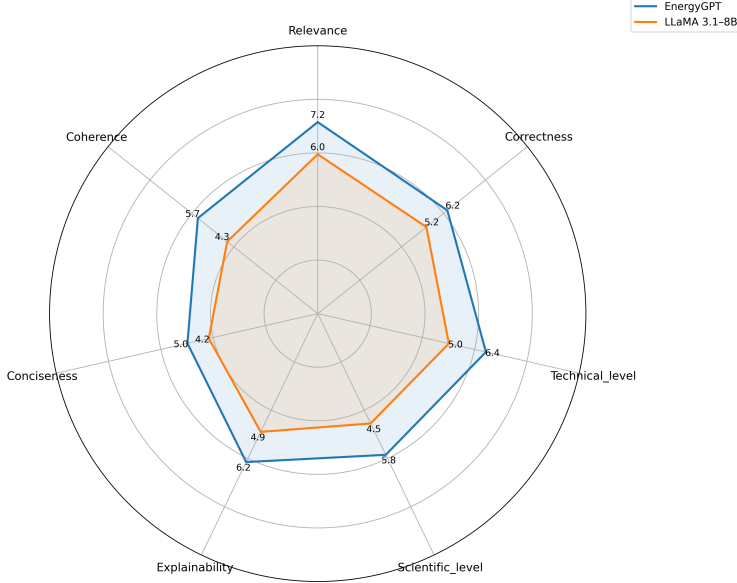


Figure 4: Radar plot of average evaluation scores.

choice or explicitly state whether a statement was true or false. Samples of the generated results by both models on multi-choice questions and true/false statements are presented in Appendix E.2 and Appendix E.3, respectively.

Question Type	No. of Questions	EnergyGPT Accuracy (%)	LLaMA 3.1-8B Accuracy (%)
Multiple-Choice Questions	233	88.0	86.0
True/False Statements	100	79	82

Table 5: Overall Accuracy on Multiple-Choice and True/False Questions.

7 EnergyGPT Deployment

To make the EnergyGPT model accessible for interactive inference and integration into downstream applications, we experimented with two deployment strategies: (1) An on-premises deployment using NVIDIA NIMs, which enabled high-throughput inference within a secure local environment. As part of this deployment, we also developed a lightweight toolkit to generate API keys, track per-user usage, handle authentication, enforces per-user quotas, and logs detailed usage statistics for monitoring and auditing. (2) A cloud-based deployment using Microsoft Azure, where we integrated the model into Azure Machine Learning (AML) Workspace. For this setup, we leveraged Azure API Management (APIM) to expose the model via REST APIs, enforce API key-based access control, and monitor usage metrics.

7.1 On Premises Deployment with NVIDIA NIMs

For secure and high-performance inference in a controlled environment, we deployed EnergyGPT on-premises using NVIDIA Inference Microservices (NIMs). NIM provides a simple and scalable mechanism to serve LLMs via standardized REST endpoints, wrapping the NVIDIA Triton Inference Server and TensorRT-LLM optimization under the hood. We used a server equipped with 4 x NVIDIA A100-SXM4-80GB GPUs. The deployment was containerized and launched using the official NIM LLaMA-3.1-8B Instruct container from NVIDIA’s NGC registry. The fine-tuned model (stored in Hugging Face format) was mounted into the container, and served using the command shown in Listing 1.

This configuration exposed the EnergyGPT model through a RESTful API endpoint, accessible at <http://localhost:8000/v1/completions>, using an OpenAI-compatible interface. The model was served with full GPU acceleration, benefiting from NVIDIA’s runtime optimizations for memory-efficient inference and prompt

```
docker run -it --rm --gpus all \
--shm-size=64g \
--ulimit memlock=-1 \
--ulimit stack=67108864 \
--network=host \
-e NGC_API_KEY=$NGC_API_KEY \
-e NIM_DISABLE_NGC_INJECTION=true \
-e NIM_FT_MODEL=/data/energygpt \
-e NIM_SERVED_MODEL_NAME=energygpt \
-v /data:/data \
nvcr.io/nim/meta/llama-3.1-8b-instruct:1.3.0
```

Listing 1: On-premises deployment of EnergyGPT using NVIDIA NIM.

caching.

To ensure secure, multi-tenant access and enforce resource quotas, we implemented a modular API gateway using FastAPI. This service acts as a proxy in front of the EnergyGPT inference endpoint, and authenticates each request via a project-specific API key provided in the `Authorization` header, enabling role-based access control across multiple organizations and projects.

API keys are uniquely issued at the project level and governed by configurable quotas, including maximum request counts and total token budgets. Upon each request, the system performs quota validation, proxies the payload to the NIM backend, parses usage metadata (e.g., prompt and completion token counts), and logs the result to a relational database. Usage is aggregated at daily, monthly, and yearly levels for each project and organization, enabling detailed metering and longitudinal analysis.

The system supports advanced key lifecycle operations, including:

- Automatic generation of API keys upon project creation.
- Seamless regeneration of keys with historical linking and soft deactivation of prior keys.
- Real-time enforcement of per-key request and token quotas.
- Tracking of last usage timestamps and project-level usage roll-ups.

Administrators of added organizations are granted access to dedicated management endpoints, allowing them to:

- Create projects and add users dynamically.
- Generate and revoke API keys, with support for seamless key regeneration and deactivation of prior keys.
- Assign request and token quotas per key or project.
- Export detailed API usage logs and key metadata in CSV format for billing, auditing, or analytics.

7.2 Deployment in Azure

We tested the deployment of a production-ready version of EnergyGPT on Microsoft Azure using a managed online endpoint within the Azure Machine Learning (AML) workspace. The model was hosted on GPU-enabled virtual machines (Standard-NV18ads-A10-v5) and served via a custom Docker image registered in Azure Container Registry (ACR), which bundled all necessary dependencies for inference. To reduce memory footprint and improve throughput, the model was quantized using 4-bit precision. Azure ML also provided built-in support for versioning, reproducibility, and dynamic resource provisioning, enabling the deployment to elastically scale with workload demands.

To securely expose the model and manage external access, the AML endpoint was integrated with Azure API Management (APIM) [60, 61], which served as an authentication and governance layer. All inference requests were routed through APIM’s centralized gateway and access to the EnergyGPT API was managed through an API product, *EnergyGPT Access*, to which each organization or internal project subscribed. Upon subscription, a unique API key was issued per project, enabling isolated and traceable access. These keys were required in all client requests and were validated using declarative, header-based policies defined within the APIM configuration, which enforced strict authentication, rejected unauthorized or anonymous traffic, and ensured consistent request formatting prior to reaching the backend endpoint.

The API gateway enforced additional policies at the inbound stage, including key validation, request header normalization, and quota enforcement. These were defined declaratively using APIM’s XML-based policy engine and applied uniformly across all requests. The policy framework also enabled advanced features such as token-based routing, header rewriting, and rate limiting for a secure and predictable service behavior.

The integration of Azure API Management (APIM) also enabled per-project usage isolation and flexible credential lifecycle management, including key regeneration and revocation. Administrators could monitor API activity through Azure Monitor and Application Insights, gaining visibility into key metrics such as request volumes, success and failure rates, and token consumption. A self-service developer portal allowed subscribed users to create and manage projects, retrieve keys, track usage, and test the model interactively. A step-by-step guide for setting up APIM can be found in Appendix F.

8 Limitations & Future Work

One key direction for future work is the integration of retrieval-augmented generation (RAG) strategies. While in this paper we benchmarks EnergyGPT against the base LLaMA 3.1-8B model on standalone question-answering tasks, we did not explore RAG-based approaches. EnergyGPT operates as a fully parametric model, relying entirely on internalized knowledge, whereas RAG systems can dynamically retrieve external information to supplement responses. Comparing these approaches would enable a comprehensive evaluation of trade-offs in accuracy, latency, and domain consistency across diverse task types, and help clarify the relative strengths of static domain specialization versus real-time retrieval capabilities.

A second open question concerns training dynamics. In this work, training was halted early based on the plateauing of validation loss; however, the optimal number of epochs required to achieve maximal domain specialization remains an open question. Future research will aim to systematically explore the relationship between training duration and downstream task performance, with the goal of identifying convergence trends and balancing the risks of underfitting and overfitting.

Third, we observed that EnergyGPT exhibited strong instruction-following behavior, particularly in multiple-choice settings, where it often returned only the answer key, as prompted. Notably, this emerged without any explicit instruction tuning. This suggests that the fine-tuning process itself may have implicitly reinforced instruction adherence, raising an interesting opportunity to study it.

Finally, a fundamental limitation of the current model lies in its lack of explicit support for multi-step reasoning. Many tasks in the energy and engineering domains demand logical chains of inference, numerical problem solving, equation handling, and causal reasoning. While EnergyGPT performs well on factual and coherent responses, it lacks structured inferential capabilities. To address this, we plan to develop a reasoning-augmented version of EnergyGPT, trained on carefully curated datasets that emphasize step-by-step analytical reasoning and evidence-based justifications, thereby enhancing the model’s ability to respond to complex, scientifically rigorous queries.

9 Conclusion

In this paper, we introduced EnergyGPT, a specialized language model for the energy sector. Our work spans the entire development pipeline, from the curation and preprocessing of domain-relevant dataset to fine-tuning, evaluation and deployment into production environment. Throughout this work, we proposed a cost-efficient and scalable approach for domain adaptation through supervised fine-tuning, offering a practical alternative to more resource-intensive methods such as training models from scratch or applying continual pretraining. We leveraged NVIDIA NeMo at multiple stages of this work, notably in The Pile data curation and in SFT process. Our results demonstrate that our fine-tuning strategy enhanced the model’s performance in domain-specific language understanding and generation. Future work will focus on extending EnergyGPT with improved reasoning capabilities, enabling it to handle more complex, multi-step analytical tasks relevant to the energy domain.

10 Acknowledgment

The authors would like to thank Dr. Kenneth Kwayu for his invaluable assistance with data collection and extraction. We also extend our gratitude to the NVIDIA Corporation Inception program and the Microsoft for Startups program for their technical support and the resources provided throughout this research.

References

- [1] Mutasim Mim. Domain specialization of large language models. Technical report, Fitila Technologies, Chicago, IL, 2023. Summer Research Associate Internal Report.
- [2] Llama Team, AI@Meta. The llama 3 herd of models. *arXiv preprint arXiv:2407.21783*, 2024. URL <https://doi.org/10.48550/arXiv.2407.21783>.
- [3] Jinhyuk Lee, Wonjin Yoon, Sungdong Kim, Donghyeon Kim, Sunkyu Kim, Chan Ho So, and Jaewoo Kang. Biobert: a pre-trained biomedical language representation model for biomedical text mining. *Bioinformatics*, 36(4):1234–1240, 2019. doi: 10.1093/bioinformatics/btz682.
- [4] Shijie Wu, Ozan rsoy, Steven Lu, Vadim Dabrowski, Mark Dredze, Sebastian Gehrmann, Prabhanjan Kambadur, David Rosenberg, and Gideon Mann. Bloomberggpt: A large language model for finance. *arXiv preprint arXiv:2303.17564*, 2023.
- [5] Nicolas Webersinke, Mathias Kraus, Julia Anna Bingler, and Markus Leippold. Climatebert: A pretrained language model for climate-related text. *arXiv preprint arXiv:2110.12010*, 2022.
- [6] Chen Ling, Xujiang Zhao, Jiaying Lu, Chengyuan Deng, Can Zheng, Junxiang Wang, Tanmoy Chowdhury, Yun Li, Hejie Cui, Xuchao Zhang, et al. Domain specialization as the key to make large language models disruptive: A comprehensive survey. *arXiv preprint arXiv:2305.18703*, 2024.
- [7] Renqian Luo, Lai Sun, Yingce Xia, Tao Qin, Sheng Zhang, Hoifung Poon, and Tie-Yan Liu. Biogpt: Generative pre-trained transformer for biomedical text generation and mining. *Briefings in bioinformatics*, 2022. URL <https://api.semanticscholar.org/CorpusID:252542956>.
- [8] Elliot Bolton, Abhinav Venigalla, Michihiro Yasunaga, David Hall, Betty Xiong, Tony Lee, Roxana Daneshjou, Jonathan Frankle, Percy Liang, Michael Carbin, and Christopher D. Manning. Biomedlm: A 2.7b parameter language model trained on biomedical text. *arXiv preprint arXiv:2403.18421*, 2024.
- [9] Ross Taylor, Marcin Kardas, Guillem Cucurull, Thomas Scialom, Anthony Hartshorn, Elvis Saravia, Andrew Poulton, Viktor Kerkez, and Robert Stojnic. Galactica: A large language model for science. *arXiv preprint arXiv:2211.09085*, 2022.
- [10] Jordan Hoffmann, Sebastian Borgeaud, Arthur Mensch, Elena Buchatskaya, Trevor Cai, Eliza Rutherford, Diego de Las Casas, Lisa Anne Hendricks, Johannes Welbl, Aidan Clark, et al. Training compute-optimal large language models. *arXiv preprint arXiv:2203.15556*, 2022. URL <https://arxiv.org/abs/2203.15556>.
- [11] Alec Radford, Jeff Wu, Rewon Child, David Luan, Dario Amodei, and Ilya Sutskever. Language models are unsupervised multitask learners. 2019. URL <https://api.semanticscholar.org/CorpusID:160025533>.
- [12] OpenAI. Gpt-4 technical report. *arXiv preprint arXiv:2303.08774*, 2023. URL <https://arxiv.org/abs/2303.08774>.
- [13] Jacob Devlin, Ming-Wei Chang, Kenton Lee, and Kristina Toutanova. Bert: Pre-training of deep bidirectional transformers for language understanding. In *North American Chapter of the Association for Computational Linguistics*, 2019. URL <https://api.semanticscholar.org/CorpusID:52967399>.
- [14] Ben Cottier, Robi Rahman, Loredana Fattorini, Nestor Maslej, Tamay Besiroglu, and David Owen. The rising costs of training frontier ai models. *arXiv preprint arXiv:2405.21015*, 2024. URL <https://arxiv.org/abs/2405.21015>.
- [15] Daixuan Cheng, Yuxian Gu, Shaohan Huang, Junyu Bi, Minlie Huang, and Furu Wei. Instruction pre-training: Language models are supervised multitask learners. *arXiv preprint arXiv:2406.14491*, 2024. URL <https://arxiv.org/abs/2406.14491>.
- [16] Suchin Gururangan, Ana Marasović, Swabha Swayamdipta, Kyle Lo, Iz Beltagy, Doug Downey, and Noah A. Smith. Don’t stop pretraining: Adapt language models to domains and tasks. In *Proceedings of the 58th Annual Meeting of the Association for Computational Linguistics*, page 83428360. Association for Computational Linguistics, 2020. URL <https://aclanthology.org/2020.acl-main.740/>.
- [17] Zixuan Ke, Yijia Shao, Haowei Lin, Tatsuya Konishi, Gyuhak Kim, and Bing Liu. Continual pre-training of language models. In *International Conference on Learning Representations*, 2023. URL <https://arxiv.org/abs/2302.03241>.
- [18] Adam Ibrahim, Benjamin Thérien, Kshitij Gupta, Mats L. Richter, Quentin Anthony, Timothée Lesort, Eugene Belilovsky, and Irina Rish. Simple and scalable strategies to continually pre-train large language models. *Transactions on Machine Learning Research*, June 2024. URL <https://openreview.net/forum?id=DimPeeCxKO>.

[19] Xisen Jin, Dejiao Zhang, Henghui Zhu, Wei Xiao, Shang-Wen Li, Xiaokai Wei, Andrew Arnold, and Xiang Ren. Lifelong pretraining: Continually adapting language models to emerging corpora. *arXiv preprint arXiv:2110.08534*, 2022. URL <https://arxiv.org/abs/2110.08534>.

[20] Tongtong Wu, Massimo Caccia, Zhuang Li, Yuan-Fang Li, Guilin Qi, and Gholamreza Haffari. Pretrained language model in continual learning: A comparative study. In *International Conference on Learning Representations*, 2022. URL <https://openreview.net/forum?id=figzpGMrdD>.

[21] Yong Xie, Karan Aggarwal, and Aitzaz Ahmad. Efficient continual pre-training for building domain specific large language models. *arXiv preprint arXiv:2311.08545*, 2023. URL <https://arxiv.org/abs/2311.08545>.

[22] Joel Jang, Seonghyeon Ye, Sohee Yang, Joongbo Shin, Janghoon Han, Gyeonghun Kim, Stanley Jungkyu Choi, and Minjoon Seo. Towards continual knowledge learning of language models. *arXiv preprint arXiv:2110.03215*, 2022. URL <https://arxiv.org/abs/2110.03215>.

[23] Joel Jang, Seonghyeon Ye, Changho Lee, Sohee Yang, Joongbo Shin, Janghoon Han, Gyeonghun Kim, and Minjoon Seo. Temporalwiki: A lifelong benchmark for training and evaluating ever-evolving language models. In *Proceedings of the 2022 Conference on Empirical Methods in Natural Language Processing*, pages 6237–6250. Association for Computational Linguistics, 2022.

[24] Aldo Pareja, Nikhil Shivakumar Nayak, Hao Wang, Krishnateja Killamsetty, Shivchander Sudalairaj, Wenlong Zhao, Seungwook Han, Abhishek Bhandwaldar, Guangxuan Xu, Kai Xu, Ligong Han, Luke Inglis, and Akash Srivastava. Unveiling the secret recipe: A guide for supervised fine-tuning small llms. *arXiv preprint arXiv:2412.13337*, 2024. URL <https://arxiv.org/abs/2412.13337>.

[25] Zixiang Chen, Yihe Deng, Huizhuo Yuan, Kaixuan Ji, and Quanquan Gu. Self-play fine-tuning converts weak language models to strong language models. In *Proceedings of the 41st International Conference on Machine Learning*, 2024. URL <https://doi.org/10.48550/arXiv.2401.01335>.

[26] Nick Mecklenburg, Yiyu Lin, Xiaoxiao Li, Daniel Holstein, Leonardo Nunes, Sara Malvar, Bruno Silva, Ranveer Chandra, Vijay Aski, Pavan Kumar Reddy Yannam, Tolga Aktas, and Todd Hendry. Injecting new knowledge into large language models via supervised fine-tuning. *arXiv preprint arXiv:2404.00213*, 2024. URL <https://arxiv.org/abs/2404.00213>.

[27] Edward J. Hu, Yelong Shen, Phillip Wallis, Zeyuan Allen-Zhu, Yuanzhi Li, Shean Wang, Lu Wang, and Weizhu Chen. Lora: Low-rank adaptation of large language models. *arXiv preprint arXiv:2106.09685*, 2021. URL <https://arxiv.org/abs/2106.09685>.

[28] Tim Dettmers, Artidoro Pagnoni, Ari Holtzman, and Luke Zettlemoyer. Qlora: Efficient finetuning of quantized llms. *arXiv preprint arXiv:2305.14314*, 2023. URL <https://arxiv.org/abs/2305.14314>.

[29] Neil Houlsby, Andrei Giurgiu, Stanisław Jastrzębski, Bruna Morrone, Quentin de Laroussilhe, Andrea Gesmundo, Mona Attariyan, and Sylvain Gelly. Parameter-efficient transfer learning for nlp. In *Proceedings of the 36th International Conference on Machine Learning*, volume 97, pages 2790–2799. PMLR, 2019. URL <https://arxiv.org/abs/1902.00751>.

[30] Zhen Li, Yupeng Su, Runming Yang, Congkai Xie, Zheng Wang, Zhongwei Xie, Ngai Wong, and Hongxia Yang. Quantization meets reasoning: Exploring llm low-bit quantization degradation for mathematical reasoning. *arXiv preprint arXiv:2501.03035*, 2025. URL <https://arxiv.org/abs/2501.03035>.

[31] Patrick Lewis, Ethan Perez, Aleksandra Piktus, Fabio Petroni, Vladimir Karpukhin, Naman Goyal, Heinrich Kütter, Mike Lewis, Wen-tau Yih, Tim Rocktäschel, Sebastian Riedel, and Douwe Kiela. Retrieval-augmented generation for knowledge-intensive nlp tasks. *arXiv preprint arXiv:2005.11401*, 2021. URL <https://arxiv.org/abs/2005.11401>.

[32] Scott Barnett, Stefanus Kurniawan, Srikanth Thudumu, Zach Brannelly, and Mohamed Abdelrazek. Seven failure points when engineering a retrieval augmented generation system. In *Proceedings of the 3rd International Conference on AI Engineering, Software Engineering for AI (CAIN 2024)*, Lisbon, Portugal, 2024. Association for Computing Machinery. URL <https://doi.org/10.1145/3644815.3644945>.

[33] Brian J. Chan, ChaoTing Chen, JuiHung Cheng, and HenHsen Huang. Dont do rag: When cache-augmented generation is all you need for knowledge tasks. 2025. doi: 10.1145/3701716.3715490. URL <https://arxiv.org/abs/2412.15605>.

[34] Leo Gao, Stella Biderman, Sid Black, Laurence Golding, Travis Hoppe, Charles Foster, Jason Phang, Horace He, Anish Thite, Noa Nabeshima, Shawn Presser, Connor Leahy, and EleutherAI. The pile: An 800gb dataset of diverse text for language modeling. *arXiv preprint arXiv:2101.00027*, 2020. URL <https://arxiv.org/abs/2101.00027>.

[35] NVIDIA. Nvidia nemo curator. <https://developer.nvidia.com/nemo-curator>, . Accessed: 2025-07-06.

[36] Tom B. Brown, Benjamin Mann, Nick Ryder, Melanie Subbiah, Jared Kaplan, Prafulla Dhariwal, Arvind Neelakantan, Pranav Shyam, Girish Sastry, Amanda Askell, Sandhini Agarwal, Ariel Herbert-Voss, Gretchen Krueger, Tom Henighan, Rewon Child, Aditya Ramesh, Daniel M. Ziegler, Jeffrey Wu, Clemens Winter, Christopher Hesse, Mark Chen, Eric Sigler, Mateusz Litwin, Scott Gray, Benjamin Chess, Jack Clark, Christopher Berner, Sam McCandlish, Alec Radford, Ilya Sutskever, and Dario Amodei. Language models are few-shot learners. *arXiv preprint arXiv:2005.14165*, 2020.

[37] HashingTF PySpark 3.4.1 documentation. <https://spark.apache.org/docs/latest/api/python/reference/api/pyspark.ml.feature.HashingTF.html>. Accessed: 2025-07-17.

[38] Project Gutenberg. URL <https://www.gutenberg.org/>. Accessed: 20250827.

[39] NVIDIA. Data curation — quality filtering. <https://docs.nvidia.com/nemo-framework/user-guide/latest/datacuration/qualityfiltering.html#data-curator-qualityfiltering>, . Accessed: 2025-07-07.

[40] NVIDIA. Quality classifier - deberta. <https://huggingface.co/nvidia/quality-classifier-deberta>, . Accessed: 2025-07-06.

[41] Guilherme Penedo, Quentin Malartic, Daniel Hesslow, Ruxandra Cojocaru, Alessandro Cappelli, Hamza AlObaidli, Baptiste Pannier, Ebtesam Almazrouei, and Julien Launay. The refinedweb dataset for falcon llm: Outperforming curated corpora with web data, and web data only. *arXiv preprint arXiv:2306.01116*, 2023. URL <https://arxiv.org/abs/2306.01116>.

[42] Kushal Tirumala, Daniel Simig, Armen Aghajanyan, and Ari S. Morcos. D4: Improving llm pretraining via document de-duplication and diversification. *arXiv preprint arXiv:2308.12284*, 2023. URL <https://arxiv.org/abs/2308.12284>.

[43] Niklas Muennighoff, Alexander M. Rush, Boaz Barak, Teven Le Scao, Aleksandra Piktus, Nouamane Tazi, Sampo Pyysalo, Thomas Wolf, and Colin Raffel. Scaling data-constrained language models. In *NeurIPS 2023 (37th Conference on Neural Information Processing Systems)*, 2023. URL <https://arxiv.org/abs/2305.16264>.

[44] Katherine Lee, Daphne Ippolito, Andrew Nystrom, Chiyuan Zhang, Douglas Eck, Chris Callison-Burch, and Nicholas Carlini. Deduplicating training data makes language models better. *arXiv preprint arXiv:2107.06499*, 2022. URL <https://arxiv.org/abs/2107.06499>.

[45] NVIDIA. Data curation — deduplication. <https://docs.nvidia.com/nemo-framework/user-guide/latest/datacuration/gpudeduplication.html>, . Accessed: 2025-07-07.

[46] Shaden Smith, Mostafa Patwary, Brandon Norick, Patrick LeGresley, Samyam Rajbhandari, Jared Casper, Zhun Liu, Shrimai Prabhumoye, George Zerveas, Vijay Korthikanti, Elton Zhang, Rewon Child, Reza Yazdani Am-inabadi, Julie Bernauer, Xia Song, Mohammad Shoeybi, Yuxiong He, Michael Houston, Saurabh Tiwary, and Bryan Catanzaro. Using deepspeed and megatron to train megatron-turing nlg 530b, a large-scale generative language model, 2022. URL <https://arxiv.org/abs/2201.11990>.

[47] Eric Zhu. Datasketch - MinhashLSH. <https://ekzhu.com/datasketch/lsh.html>. Accessed: 2025-07-17.

[48] Jure Leskovec, Anand Rajaraman, and Jeffrey D. Ullman. *Mining of Massive Datasets*. Cambridge University Press, 3rd edition, 2020.

[49] Amro Abbas, Kushal Tirumala, Dániel Simig, Surya Ganguli, and Ari S. Morcos. Semdedup: Data-efficient learning at web-scale through semantic deduplication. *arXiv preprint arXiv:2303.09540*, 2023. URL <https://arxiv.org/abs/2303.09540>.

[50] Nils Reimers and Iryna Gurevych. Sentence-bert: Sentence embeddings using siamese bert-networks. In *Proceedings of the 2019 Conference on Empirical Methods in Natural Language Processing*, pages 3982–3992. Association for Computational Linguistics, 2019. doi: 10.18653/v1/D19-1410. URL <https://aclanthology.org/D19-1410>.

[51] intfloat. e5-large-v2. <https://huggingface.co/intfloat/e5-large-v2>. Accessed: 2025-07-07.

[52] Beijing Academy of Artificial Intelligence (BAAI). Baai general embedding (bge) base english v1.5. <https://huggingface.co/BAAI/bge-base-en-v1.5>. Accessed: 2025-07-07.

[53] Sentence Transformers. all-mpnet-base-v2. <https://huggingface.co/sentence-transformers/all-mpnet-base-v2>. Accessed: 2025-07-07.

[54] Zheng Zhang, Chen Zheng, Da Tang, Ke Sun, Yukun Ma, Yingtong Bu, Xun Zhou, and Liang Zhao. Balancing specialized and general skills in llms: The impact of modern tuning and data strategy, 2023. URL <https://arxiv.org/abs/2310.04945>.

- [55] Yun Luo, Zhen Yang, Fandong Meng, Yafu Li, Jie Zhou, and Yue Zhang. An empirical study of catastrophic forgetting in large language models during continual fine-tuning, 2025. URL <https://doi.org/10.48550/arXiv.2308.08747>.
- [56] Mohammad Shoeybi, Mostofa Patwary, Raul Puri, Patrick LeGresley, Jared Casper, and Bryan Catanzaro. Megatron-Lm: Training multi-billion parameter language models using model parallelism. *arXiv preprint arXiv:1909.08053*, 2019. URL <https://arxiv.org/abs/1909.08053>.
- [57] Deepak Narayanan, Mohammad Shoeybi, Jared Casper, Patrick LeGresley, Mostofa Patwary, Vijay Korthikanti, Reza Aminabadi, Bryan Catanzaro, and Matei Zaharia. Efficient large-scale language model training on gpu clusters using megatron-lm. *arXiv preprint arXiv:2104.04473*, 2021. URL <https://arxiv.org/abs/2104.04473>.
- [58] Lianmin Zheng, Wei-Lin Chiang, Ying Sheng, Siyuan Zhuang, Zhanghao Wu, Yonghao Zhuang, Zi Lin, Zhuohan Li, Dacheng Li, Eric P Xing, et al. Judging llm-as-a-judge with mt-bench and chatbot arena. *arXiv preprint arXiv:2306.05685*, 2023. URL <https://doi.org/10.48550/arXiv.2306.05685>.
- [59] Ge Bai, Jie Liu, Xingyuan Bu, Yancheng He, Jiaheng Liu, Zhanhui Zhou, et al. Mt-bench-101: A fine-grained benchmark for evaluating large language models in multi-turn dialogues. *arXiv preprint arXiv:2402.14762*, 2024. URL <https://doi.org/10.48550/arXiv.2402.14762>.
- [60] Microsoft Learn. *API Management documentation*, 2025. <https://learn.microsoft.com/en-us/azure/api-management/>. Accessed: 2025-07-07.
- [61] Microsoft Learn. *Azure API Management - Overview and key concepts*, 2025. <https://learn.microsoft.com/azure/api-management/api-management-key-concepts>. Accessed: 2025-07-07.

A Data Preprocessing

A.1 Deduplication

Jaccard Similarity

The Jaccard Similarity between two sets S and T is defined as:

$$J(S, T) = \frac{|S \cap T|}{|S \cup T|}$$

This metric quantifies the degree of overlap between two sets as the ratio of the size of their intersection to the size of their union. The value of $J(S, T)$ lies in the range $[0, 1]$, where:

- $J(S, T) = 1$ indicates that the sets are identical,
- $J(S, T) = 0$ indicates that the sets are disjoint,
- Values closer to 1 indicate greater similarity.

In the context of document similarity, the sets S and T often represent collections of features such as character-level or word-level n -grams (shingles) extracted from the documents.

MinHash

For a positive integer k , a *k-shingle* of a document D is any contiguous substring of D of length k . Each document can thus be represented as a multiset (or set) of k -shingles.

We construct a binary incidence matrix M where:

- Each row corresponds to a unique k -shingle in the corpus,
- Each column corresponds to a document,
- The entry $M_{r,c} = 1$ if the k -shingle in row r appears in document c , and 0 otherwise.

Let π be a random permutation of the row indices of M . The MinHash value of a document D under permutation π , denoted $h_\pi(D)$, is the index of the first row (i.e., the first shingle under π) where $M_{r,D} = 1$:

$$h_\pi(D) = \min \{\pi(r) \mid M_{r,D} = 1\}.$$

Proposition. For two documents D and E , the probability that their MinHash values are equal under a random permutation is equal to their Jaccard similarity:

$$\Pr[h_\pi(D) = h_\pi(E)] = J(D, E).$$

To approximate this probability, we generate n independent random permutations π_1, \dots, π_n and compute the MinHash signature vector for each document:

$$\text{sig}(D) = (h_{\pi_1}(D), h_{\pi_2}(D), \dots, h_{\pi_n}(D)).$$

For two documents D and E , the fraction of positions in which their signatures match approximates their Jaccard similarity:

$$\frac{1}{n} \sum_{i=1}^n \mathbb{I}[h_{\pi_i}(D) = h_{\pi_i}(E)] \approx J(D, E).$$

This signature provides a compact, lower-dimensional representation of the original document while preserving pairwise Jaccard similarities, enabling efficient near-duplicate detection and clustering.

In practice, generating true permutations of rows is computationally expensive. Instead, a family of hash functions $h_i : \mathbb{Z} \rightarrow \{1, 2, \dots, m\}$, where m is the number of rows in M , is used to simulate random permutations.

Locality Sensitive Hashing (LSH)

Locality Sensitive Hashing (LSH) is a technique for efficiently identifying similar pairs of items in high-dimensional spaces. When combined with MinHash signatures, LSH enables the detection of near-duplicate sets (or documents) without exhaustively computing pairwise similarities.

The core idea is to amplify the distinction between similar and dissimilar pairs by organizing MinHash signatures into a structured arrangement. Given a MinHash signature of length n , we divide it into b *bands*, each containing r rows, such that $n = b \cdot r$. Within each band, the r -row sub-vectors of the signature are hashed into buckets.

Two documents are considered candidate duplicates if they hash to the same bucket in at least one band that is, their sub-signatures are identical in that band.

Collision Probability. Let $s \in [0, 1]$ denote the Jaccard similarity between two documents. The probability that their sub-signatures match in all r rows of a given band is s^r , and the probability that they do *not* match in that band is $1 - s^r$. The probability that they fail to match in all b bands is:

$$(1 - s^r)^b.$$

Therefore, the probability that two documents are identified as candidate duplicates by LSH is:

$$P_{\text{LSH}}(s) = 1 - (1 - s^r)^b.$$

This function exhibits a sharp threshold behavior: documents with similarity above a chosen threshold are likely to be detected, while dissimilar documents have a low probability of collision. By tuning the parameters r and b , one can balance false positives and false negatives.

B Semantic Filtering Reference Topics

The following list summarizes a sample of the main topics covered in the curated reference queries used to guide semantic filtering of The Pile dataset.

- **Energy Systems and Infrastructure:** power grids, smart grids, microgrids, sector coupling.
- **Renewable Energy Sources:** solar, wind, hydropower, geothermal, biomass, ocean energy.
- **Fossil Fuels:** coal, oil, petroleum, natural gas, exploration, extraction, refining.
- **Nuclear Energy:** fission reactors, small modular reactors, nuclear fusion, waste management.
- **Hydrogen Economy:** production, storage, transport, fuel cells, industrial and transport applications.
- **Energy Policy and Economics:** climate policy, carbon pricing, subsidies, energy market structures.
- **Industrial Energy Systems:** combined heat and power, decarbonization, process electrification.
- **Carbon Management:** carbon capture, direct air capture, CCUS.
- **Emerging Technologies:** AI in energy, blockchain, advanced materials, next-generation photovoltaics.
- **Energy Science and Engineering:** thermodynamics, heat engines, gas turbines, energy physics, chemical systems.
- **Energy Efficiency and Conservation:** building efficiency, behavioral change, efficient systems.
- **Environmental Impacts:** emissions, ecosystem effects, sustainability assessments.
- **Energy Production and Consumption:** conversion processes, consumption patterns, efficiency metrics.
- **Energy Storage Systems:** batteries, thermal storage, mechanical storage, hydrogen storage.
- **Grid Integration of Renewables:** balancing, smart inverters, interconnection, stability.
- **Energy in Biological Systems:** bioenergy, biomass utilization.

C Training Infrastructure and Optimization

To optimize computational efficiency and training stability, we use an optimized training infrastructure.

Optimizer: In the training, We use the Adam optimizer with $\beta_1 = 0.9$ and a reduced $\beta_2 = 0.95$. Lowering β_2 decreases the influence of long-term gradient variance, enabling the optimizer to adapt more responsively to recent updates.

Batching and Gradient Accumulation: To support stable training and effective utilization of GPU memory, we employed gradient accumulation to achieve the desired global batch size without exceeding hardware limits. This technique allows for the accumulation of gradients over several micro-batches before performing a single optimization step, thereby simulating a larger effective batch size while maintaining manageable memory usage per device. In our configuration, each GPU processed a micro-batch of 8 samples per forward-backward pass. By accumulating gradients over multiple steps and leveraging tensor parallelism across 4 GPUs, we achieved a global batch size of 256 samples. This strategy enabled us to maintain a high throughput while preventing memory overflow on the A100-80GB GPUs. The effective batch size B is given by:

$$B = b * k * N \quad (1)$$

where b is the micro-batch size per GPU, k is the number of accumulation steps, and N is the number of GPUs used in training.

Efficient Tensor Parallelism: To enable the training of a large model on a limited number of GPUs, we utilized Tensor Parallelism (TP) to partition the model across devices at the level of individual tensor operations. Specifically, we adopted a TP size of 4, corresponding to the number of A100-80GB GPUs available in our compute cluster. Tensor Parallelism allows layers, particularly the attention and feedforward modules, to be split along their hidden dimensions, with each GPU computing a fraction of the operation and exchanging partial results via high-speed interconnects. This intra-layer parallelism strategy significantly reduces per-device memory requirements and enables training models that would otherwise exceed the memory capacity of a single GPU.

Validation Loss: In large language models, the validation loss is typically computed using the cross-entropy loss function over a sequence of tokens. Given a validation dataset $D_{\text{val}} = \{(x^{(i)}, y^{(i)})\}_{i=1}^N$, where $x^{(i)}$ is the input context and $y^{(i)}$ is the target token, the average validation loss is defined as:

$$\mathcal{L}_{\text{val}} = -\frac{1}{N} \sum_{i=1}^N \log p_{\theta} (y^{(i)} | x^{(i)}) \quad (2)$$

For autoregressive language modeling, where the task is to predict the next token in a sequence, the loss over a tokenized sequence $\{t_1, t_2, \dots, t_T\}$ is given by:

$$\mathcal{L}_{\text{val}} = -\frac{1}{T} \sum_{t=1}^T \log p_{\theta} (t_t | t_1, t_2, \dots, t_{t-1}) \quad (3)$$

Here, $p_{\theta}(\cdot)$ denotes the model's predicted probability distribution parameterized by θ , and T is the total number of tokens in the validation set. This loss quantifies how well the model predicts the next token in context and is commonly reported during training as an indicator of generalization.

The validation Loss is often converted into **perplexity**, which can be thought of as the average branching factor or the model's uncertainty in choosing the next token.

Perplexity is defined as the exponential of the cross-entropy loss:

$$\text{Perplexity} = \exp(\mathcal{L}_{\text{val}}) \quad (4)$$

A lower perplexity indicates better language modeling performance, as it implies the model is more confident and accurate in its predictions. For example, a perplexity of 1 corresponds to perfect prediction, while higher values reflect increasing uncertainty or error.

D EnergyGPT Benchmark: Samples

Sample of True/False Statements

Question 1:

Newton's first law of motion states that an object at rest will remain at rest unless acted upon by an external force.

Answer: True

Question 2:

Ionic bonds involve the transfer of electrons between atoms to form ions.

Answer: True

Question 3:

The Boltzmann constant relates the average kinetic energy of gas particles to the temperature of the gas.

Answer: False

Question 4:

CCS involves capturing CO_2 emissions from industrial processes and storing them underground in geological formations.

Answer: True

Question 5:

Enhanced oil recovery (EOR) is a process that utilizes CO_2 injection to increase oil production from reservoirs.

Answer: True

Text Box 1: Sample from the True/False Statements benchmark.

Tiered Difficulty Energy Questions

Easy Questions:

- What is the primary source of energy for Earth's climate system?
- How do wind turbines generate electricity from wind?
- What is the basic principle behind hydroelectric power generation?
- What is energy efficiency, and why does it matter in everyday appliances?

Medium Question:

- Explain how nuclear fission produces energy in a nuclear reactor.
- What are biofuels, and how do they compare to traditional fossil fuels in terms of emissions and sustainability?
- Explain the concept of energy return on investment (EROI) and its significance in evaluating energy sources.
- How does tidal energy work, and what are its potential environmental impacts?
- Discuss the advantages and limitations of using hydrogen as an alternative fuel source.

Hard Questions:

- How can perovskite materials be engineered to improve the efficiency and stability of next-generation solar cells?
- What are the potential risks and benefits of large-scale geoengineering projects aimed at mitigating climate change?
- Explain how the second law of thermodynamics limits the efficiency of various energy conversion systems, such as engines and refrigerators.
- How do quantum mechanical effects influence the performance of advanced photovoltaic materials?
- Evaluate the potential of nanotechnology in enhancing the energy storage capacity and charging speeds of supercapacitors.
- Discuss the challenges and potential solutions for carbon capture and storage technologies in reducing atmospheric CO_2 levels.

Challenging Questions:

- How can genetic engineering of microorganisms be optimized to increase the yield and reduce the production costs of advanced biofuels, and what are the ecological risks associated with deploying such organisms at scale?
- What innovative approaches are being researched for the long-term storage or neutralization of nuclear waste, and how do they compare in terms of safety, cost, and public acceptance?
- What are the latest developments in harvesting energy from ambient sources like radiofrequency waves, vibrations, or temperature differentials, and how can these technologies be optimized for powering low-energy devices?
- How is artificial intelligence being used to optimize energy consumption and distribution in smart grids, and what are the cybersecurity risks associated with increased digitalization?

Fact-Based Questions:

- What are the precise parameters (temperature and pressure) achieved in the most recent successful fusion experiment at the ITER facility?
- What is the exact cost per kilowatt-hour (kWh) of producing green hydrogen using the latest electrolysis technology as reported in a 2023 industry analysis?
- How many electric vehicles (EVs) were sold worldwide in 2022, and what percentage increase does this represent over 2021 sales figures?
- List the top five countries in lithium production for 2022, including the exact amounts produced in metric tons.
- What are the detailed outcomes of the 2022 United Nations Climate Change Conference (COP27) regarding international commitments to phase out coal-fired power plants?

Text Box 2: Sample questions covering basic to advanced energy-related concepts and factual recall.

Sample Questions: Multiple Choice Q & A

Question 1:

Which renewable energy technology uses the energy of ocean waves to generate electricity?

- A) Wave power
- B) Tidal power
- C) Hydropower
- D) Ocean thermal energy conversion

Answer: A

Question 2:

What is the term for the process of converting biomass into liquid fuels through the action of microorganisms?

- A) Biomass liquefaction
- B) Biomass gasification
- C) Biomass fermentation
- D) Biomass pyrolysis

Answer: C

Question 3:

What is the concept of the circular economy in sustainable development?

- A) Continuing the linear 'take-make-dispose' model
- B) Promoting resource conservation and reuse
- C) Ignoring environmental impacts
- D) Maximizing resource extraction

Answer: B

Question 4:

Which of the following is an example of an endothermic reaction?

- A) Combustion of gasoline
- B) Photosynthesis
- C) Formation of rust
- D) Freezing of water

Answer: B

Text Box 3: Sample questions from the multiple choice Q & A benchmark.

E EnergyGPT Benchmark: Sample Responses

E.1 Sample responses to open-ended queries

Query: How does the interaction between rotor and stator (impeller and diffuser) in pumps or turbines influence the overall hydrodynamic forces, and what are the implications for energy systems such as hydropower or industrial fluid systems?

EnergyGPT Response:

The interaction of impellers with their casing is a major source of losses. The flow field around an impeller can be divided into three regions: 1) A region close to the blade surface where viscous effects dominate; 2) An intermediate region where both pressure gradients and viscosity play important roles; and 3) A far-field region dominated by inviscid potential theory. In general, it has been found that the main loss mechanisms occur within the first two regions. For example, when considering axial turbomachinery, the tip leakage flows at the shroud clearance gap have been shown to contribute significantly towards total losses. Similarly, secondary flows near the hub and shroud end-walls also make significant contributions to losses. These phenomena are all related to interactions between the rotating blades and stationary components. As such, they will depend on factors like rotational speed, Reynolds number, etc. Furthermore, these interactions may vary depending upon whether we consider centrifugal or axial machines. Therefore, understanding how the interaction between rotors and stators affects overall performance requires careful consideration of specific geometries and operating conditions. Additionally, recent advances in computational methods allow us to investigate complex flow fields more accurately than ever before. This enables engineers to better understand loss generation processes associated with rotor-stator interactions so that improvements can be made through design modifications.

LLaMA 3.1-8B Response:

The interaction of a rotating impeller with its surrounding stationary components is crucial to understanding how these devices function. The flow field around an impeller can be complex due to interactions like secondary flows caused by centrifugal effects on vortices generated within it; this leads not only into increased losses but also affects performance characteristics significantly.

In order to better understand these phenomena we need more detailed information about their nature which requires advanced computational methods capable of capturing all relevant aspects at once - something that traditional CFD approaches struggle with because they lack sufficient resolution near walls where most important physics takes place! This article will explore some recent developments towards achieving higher fidelity simulations while still maintaining reasonable runtimes suitable even when applied across large domains typical found inside turbomachinery applications today

Introduction

Turbine blades play a vital role in converting kinetic energy from moving fluids into mechanical work. They do so through two main mechanisms: lift force generation via pressure differences created along blade surfaces, and drag reduction achieved by minimizing frictional resistance against air molecules passing over them during rotation. In addition to providing thrust power output directly proportional to rotational speed squared times area swept out per revolution multiplied by density difference between inlet/outlet streams respectively; turbine efficiency depends heavily upon proper design considerations including shape optimization techniques used throughout industry standards worldwide!

Turbine Blade Design Considerations

When designing new types of turbines there's no one-size fits-all approach since each application has unique requirements based off factors such as available space constraints imposed by existing infrastructure limitations etc., however certain general guidelines exist regardless whether you're working with small scale models intended solely for educational purposes up until full-scale commercial installations meant primarily generate electricity rather than just heat water supply needs alone. Herein lies another reason why engineers must take great care selecting materials appropriate enough withstand high temperatures without degrading too quickly otherwise risk losing valuable resources invested upfront before any significant returns could ever materialize down line later stages production cycle life spanned several decades depending project scope size complexity involved.

Query: How does integrating energy generation technologies, such as combining a fuel cell with a micro gas turbine, improve system efficiency, reduce emissions, and optimize overall energy conversion in hybrid systems?

EnergyGPT Response:

The integration of different types of power generating devices can lead to improved efficiencies. For example, the combination of a solid oxide fuel cell (SOFC) with a micro-gas-turbine (MGT), which is also known as an SOFC-MGT or MCFC-MGT configuration, has been shown to increase total system efficiency by 10-15% compared to using either device alone. This increased efficiency comes from several factors: The high temperature exhaust gases produced by the MGT are used to heat up the incoming air for the SOFC before it enters the combustor section; this preheating process reduces thermal losses that would otherwise occur if all of the hot exhaust were simply released into the atmosphere. Additionally, since both devices operate at relatively low temperatures (<1000°C), they do not require expensive materials like those needed for higher temperature applications (>1200°C). Finally, because each component operates independently but together produces more output than when operating separately, there is potential for greater control over how much electricity is generated depending on demand levelsthis could help lower costs associated with peak load times where prices tend to be highest due to limited supply availability. Overall then, these integrated systems offer better performance while reducing environmental impact through reduced emissions and improved resource utilization.

LLaMA 3.1-8B Response:

Hybridization of different power generating units can be done to achieve the following objectives:

1. To increase the total output from the combined unit.
2. To make use of waste heat available at one stage for improving the performance of another component.
3. To utilize the by-products generated during operation of any particular device.

For example: A diesel engine is used alongwith an alternator which converts mechanical work into electrical energy. The exhaust gases are utilized in a steam generator where they provide thermal energy required for raising steam. This steam drives a turbo-alternator set that generates electricity. Thus, we have three stages of energy conversion (chemical mechanical electric) taking place simultaneously. In this case, there will not only be increased production but also utilization of otherwise wasted energy. The main advantage of using multiple devices together lies in their complementary nature i.e., each device has its own advantages over others under certain operating conditions. For instance, when load demand increases beyond what can be met by just one type of prime mover alone then it becomes necessary to add more generators or engines etc.. However, if these additional machines were operated independently without coordination between them then there would likely be significant losses due to inefficiencies caused by mismatched timing cycles among all components involved.

Query: Explain how temperature and pressure interplay in a gas-driven oil-displacement process, and describe which thermodynamic equations govern the phase behavior of injected gas in a porous medium?

EnergyGPT Response:

The injection of supercritical CO_2 into an underground reservoir to recover additional crude oil is known as carbon dioxide flooding. The density of liquid hydrocarbons decreases with increasing temperature at constant pressure (ideal gas law), whereas it increases with decreasing pressure at constant temperature. Therefore, if we inject hot pressurized CO_2 into a cold subterranean formation containing heavy viscous oil, then the viscosity of the displaced fluid will decrease due to heating by the injected gas. This effect can be described using the following equation:

$$\mu_o = \frac{a}{T^b}$$

where μ is the dynamic viscosity, T is absolute temperature, and a and b are constants that depend on the specific properties of the oil being produced. In addition, the solubility of gases generally increases with both increasing temperature and pressure; however, this trend does not always hold for all types of fluids under consideration. For example, the solubility of methane in water actually

decreases slightly when its temperature exceeds 100 °C because some of the dissolved CH_4 comes out of solution as free gas bubbles instead of remaining completely dissolved within the aqueous phase. However, even though there may be exceptions like these two examples show us, most often higher temperatures tend to increase the amount of any given substance present either entirely or partially dissolved inside another material such as oil or brine found deep below ground level.

LLaMA 3.1-8B Response:

The following equation describes the relationship between temperature (T), pressure (P) and volume (V):

$$PV = nRT$$

where R is the universal gas constant. The above equation can be rearranged to give

$$\frac{1}{n} (PV) = RT$$

This expression shows that for an ideal gas at fixed T , $P \propto V$.

For example, if we consider 1000 moles of methane with a molar mass of 16 g/mol, then its molecular weight would be 16000 g/mole or 16 kg/kmol. If this amount were compressed from atmospheric conditions ($\sim 101325 Pa$) into a cylinder having a cross-sectional area of 10 cm² and length L, it could occupy volumes ranging from about 5106 mm³ up to approximately 8107 mm³ depending upon whether one uses Boyle's law ($PV=nRT$) or Charles' law ($T \propto V$). In either case though, the final result will always remain within these limits because there exists no way to compress more than twice as much matter per unit volume without violating conservation laws such as those governing energy transfer during compression/expansion processes like Joule-Thomson effect etc..

Query: Explain how gas-phase chemical kinetics interact with soot precursor formation and surface growth mechanisms, and outline the key reactions you'd include in a reduced chemical mechanism for engine-combustion simulations?

EnergyGPT Response:

The oxidation of fuel molecules to form CO_2 is not the only reaction that occurs during combustion. Other species are formed as intermediates before complete conversion into carbon dioxide or other products (such as water). These intermediate species can also react further to produce soot precursors such as acetylene (C_2H_2), which then go on to nucleate new particles through condensation processes. The rate at which these reactions occur depends on several factors including temperature, pressure, equivalence ratio, etc., but they all play an important role in determining the final composition of exhaust gases from engines. In order to accurately model this complex chemistry within computational fluid dynamics (CFD) software packages used by engineers designing internal combustion engines, it's essential to understand both the underlying physical principles governing each individual reaction step as well as their interactions with one another. This requires developing detailed kinetic models consisting of hundreds or even thousands of elementary reactions involving dozens of different molecular species. However, due to limitations imposed by computer processing power and memory capacity, it isn't always feasible to solve every single possible reaction pathway simultaneously using full-kinetic modeling approaches. Instead, many researchers have focused on reducing the complexity of these mechanisms while still capturing the most relevant aspects related to soot production. One common strategy involves grouping together multiple steps into lumped-reactions based on similar characteristics like activation energy barriers or product distributions. By doing so, we're able to represent entire classes of reactions with just a few simplified equations without losing too much accuracy when compared against more comprehensive models. For example, instead of tracking every individual hydrogen atom transfer between two adjacent hydrocarbon radicals, we might use a generic hydrogen abstraction reaction to describe any number of equivalent pathways leading up to that same end result. While there will inevitably be some trade-offs made in terms of predictive capability depending upon what specific details get sacrificed along the way, simplifying our chemical mechanisms allows us to run larger-scale CFD simulations over longer periods of time than would otherwise be possible if trying to account for everything down to the atomic level. Ultimately though, whether or not such reductions prove useful ultimately comes down to experimental validation - i. e., seeing how closely observed results match those predicted by numerical calculations incorporating various levels of detail regarding the involved chemical kinetics.

LLaMA 3.1-8B Response:

The oxidation of fuel molecules is an important process that occurs during combustion. The products of this reaction are typically carbon dioxide (CO₂) and water vapor (H₂O). However, under certain conditions such as high temperatures or low oxygen concentrations, incomplete burning can occur which leads to the production of other compounds like methane (CH₄), ethane (C₂H₆), propane (C₃H₈), butane (C₄H₁₀), pentanes (C₅H₁₂), hexanes (C₆H₁₄), heptanes (C₇H₁₆), octanes (C₈H₁₈), nonanes (C₉H₂₀), decanes (C₁₀H₂₂), undecanes (C₁₁H₂₄), dodecane (C₁₂H₂₆), tridecenes (C₁₃H₂₈), tetradecenes (C₁₄H₃₀), pentadecenes (C₁₅H₃₂), hexadecenes (C₁₆H₃₄), heptadecenes (C₁₇H₃₆), octadecenes (C₁₈H₃₈), nonadecenes (C₁₉H₄₀), eicosene (C₂₀H₄₂), hentriacontane (C₃₁H₆₄), dotriacontane (C₃₂H₆₆), tetratriacontane (C₃₄H₇₀), pentacontane (C₃₅H₇₂), hexatetracontane (C₃₇H₇₆), heptaheptacosa-1-ene (C₃₉H₇₈), octaoctacosanone (C₄₁H₈₂), ennonononaenol (C₄₃H₈₆), decahexadecaenyl acetate (C₄₅H₉₀), undecaundecanoic acid methyl ester (C₄₇H₉₄), dodecadodecanoic acid dimethyl ether (C₄₉H₉₈), triethylenediamine dihydrochloride monohydrate (C₅₀H₁₀₀N₂Cl₂ H₂O), tetramethylene sulfite oxide hydrate (C₅₂H₁₀₄S₂O₂ 0.25H₂O), pentamethylene disulfide bis(trifluoromethylsulfonyl)imide salt (C₅₄H₁₀₈F₆NS₄S₂), hexamethylene selenoxide sesquiselenocyanate (C₅₆H₁₁₂Se₃CN₆), heptamethylene tellurium dichloro

Query: Design a multi-zone combustion simulation framework that uses adaptive mesh refinement to capture steep temperature and concentration gradients, and discuss how you'd validate each zone's solution against experimental data?

EnergyGPT Response:

To design a multi-zone combustion simulation framework using adaptive mesh refinement (AMR) to capture steep temperature and concentration gradients, one would need to consider several factors. Here is an outline of the steps involved in designing such a framework:

- 1 - Problem Definition:** Clearly define the problem statement for which this simulation framework will be used. This includes understanding the physical processes involved in combustion, as well as any specific goals or objectives associated with the study. For example, if studying engine combustion, it may involve modeling multiple zones including intake manifold, cylinder, exhaust system etc., all interacting through fluid dynamics equations like Navier-Stokes equation coupled with chemical kinetics models.
- 2 - Numerical Methodology:** Choose appropriate numerical methods and algorithms suitable for solving complex multiphase flow problems involving heat transfer, mass transport & reaction chemistry simultaneously across different spatial scales. In particular, AMR can help refine local regions where large gradients exist without wasting computational resources on areas having smooth solutions. A common approach involves discretizing governing partial differential equations over finite volumes/elements followed by iterative solution techniques like Gauss-Seidel method, conjugate gradient method etc.. Additionally, turbulence closure models are often employed to account for eddy viscosity effects arising due to chaotic nature of turbulent flows encountered during combustion process.
- 3 - Model Formulation:** Based upon the chosen numerical methodology, formulate mathematical model describing conservation laws of mass, momentum, energy along with species transport equations incorporating relevant submodels for turbulence, radiation, ignition delay time etc. Depending upon complexity level desired, simplified versions of these equations could also be considered depending upon availability of accurate reduced mechanisms for given fuel-air mixture under consideration.
- 4 - Code Development:** Implement aforementioned formulations into computer code utilizing object-oriented programming paradigm so that individual components responsible for handling distinct aspects of overall physics can easily be replaced or extended later when required. Utilize parallel computing capabilities wherever possible since simulations involving reacting flows tend to become computationally intensive very quickly owing to stiff ordinary differential equations resulting from chemical kinetic rates.
- 5 - Verification & Validation:** Once complete implementation has been achieved, verify correctness of developed codes via analytical test cases available in literature while validating them further against experiments conducted specifically for same set of conditions being simulated. Pay special attention towards ensuring accuracy of results obtained near boundaries separating adjacent zones especially those characterized by sharp changes in thermodynamic properties leading to formation of shock waves.

LLaMA 3.1-8B Response:

The design of an efficient and accurate numerical model for simulating the behavior of multiple zones in a combustion system is crucial. The key challenge lies in capturing sharp changes in both temperature and species concentrations while ensuring computational efficiency. To address this issue, we propose using Adaptive Mesh Refinement (AMR) techniques within our proposed Multi-Zone Combustion Simulation Framework. AMR allows us to dynamically refine or coarsen meshes based on local error estimates, resulting in more precise solutions with fewer grid points overall compared to uniform grids alone. In order to ensure accuracy across all zones, it will be necessary to compare results obtained from simulations conducted at different levels of resolution against available experimental measurements. This validation process can help identify any potential sources of errors introduced by simplifying assumptions made during modeling such as turbulence models used or boundary conditions imposed upon individual regions within the domain being simulated. By carefully selecting appropriate experiments which provide sufficient information about relevant physical phenomena occurring inside these domains e.g., flame speed profiles etc.. one could gain confidence regarding reliability & applicability range(s) associated w/ particular implementation choices taken whilst developing said software package itself! Additionally, post-processing tools like contour plots showing spatial variations over time may also prove useful when analyzing output generated via aforementioned approach(es).

Query: What seismic-inversion techniques are used to estimate porosity and fluid saturation in deep coal seams, and how are they validated against well-log data?

EnergyGPT Response:

Seismic inversion is a technique that uses prestack seismic data to determine rock properties such as acoustic impedance (AI), shear impedance (SI) or elastic stiffnesses. The method involves the use of an earth model with known petrophysical parameters for which synthetic seismograms can be generated using forward modeling. These synthetic traces are compared with field observations, and by minimizing differences between them, the best possible values of unknown rock properties are determined. In this study we present two different approaches to invert prestack seismic data over a thick sequence of coals from the Walloon Coal Measures in the Surat Basin, Queensland, Australia. We compare results obtained through conventional AVO inversion and simultaneous inversion of AI and SI logs. Both methods were able to reproduce laboratory-measured P-impedance trends along wells; however, only the latter was capable of reproducing S-impedance patterns observed at one location where core samples were available. This suggests that both AI and SI need to be considered when characterizing reservoirs composed mainly of organic matter. Furthermore, our analysis shows that the presence of gas within the coal matrix causes significant changes on the lithostatic compressibility of the rocks, resulting in large variations of the estimated rock density. Finally, we demonstrate that it is possible to obtain reliable estimates of water saturations in these formations based solely on inverted log data.

LLaMA 3.1-8B Response:

Seismic inversion is a technique that uses the relationship between rock properties (such as density or acoustic impedance) and seismic wave velocities. This allows us to convert seismic amplitudes into estimates of these physical parameters.

The most common method for estimating porosity from seismic data involves using an empirical equation called Gardner's law which relates bulk density (ρ_b), grain density (ρ_g), and pore space fraction(porosity)(ϕ):

$\rho_b = \rho_g(1 - \phi)^2 + \rho_f\phi$ where ρ_f represents the density of fluids within pores. In order to apply this formula we need information about both ρ_g and ρ_f which can be obtained through laboratory measurements on core samples taken during drilling operations. Once these values have been determined then Equation 1 provides us with an expression linking measured densities at different depths along our borehole trajectory back up towards surface where no direct measurement exists due lack of penetration depth by drill bit etc.. However there may still remain some uncertainty associated with exact value chosen since it depends upon many factors including lithology composition mineralogy texture degree weathering etc... Therefore alternative approaches exist such as statistical regression analysis whereby multiple variables affecting porosity e.g., shale content clay minerals organic matter type etc...,are considered simultaneously rather than just one single factor alone

Query: Outline an optimization workflow for minimizing particulate emissions in a compression-ignition engine by tuning injection timing, pressure, and exhaust-after treatment parameters, and describe how you'd quantify trade-offs between soot mass and particle count?

EnergyGPT Response:

- Define the objective function to be minimized:

$$\begin{aligned} \min \quad & J = w_1 m_{\text{soot}} + w_2 n_{\text{particles}} \\ \text{subject to} \quad & w_1, w_2 > 0, \quad w_1 + w_2 = 1 \end{aligned}$$

Here m_{soot} is the total soot mass emitted over some time period (e. g., one driving cycle), while $n_{\text{particles}}$ is the number of particles counted during that same time interval. The weights w_1 and w_2 allow us to tune the relative importance of these two terms. For example, if we are more concerned with reducing the overall amount of soot than limiting the maximum number of particles per unit volume, then we would set $w_1 > w_2$. In general, it may also be desirable to consider other factors such as fuel economy or NOx production when optimizing this system but those will not be considered here. Note that there could potentially be additional constraints on the problem for instance, limits on the range of values each parameter can take, or bounds on their derivatives (i. e., rates at which they change). However, since no such restrictions apply in our case study below, none have been included.

LLaMA 3.1-8B Response:

This is the first of two posts on this topic. In Part 1, I'll outline my approach to solving this problem using MATLAB. Then, in Part 2, we will look at some results.

Problem Statement.

The goal here is to minimize particulate matter (PM) from diesel engines while maintaining acceptable performance metrics such as fuel economy or power output. The PM consists primarily of carbonaceous particles that are emitted during combustion. These particles can be harmful if they enter the lungs because their small size allows them to penetrate deep into lung tissue where they may cause inflammation and other health problems [1].

To achieve these goals, engineers must optimize several factors related to both the design of the engine itself and its operation under different conditions. For example, one way to reduce PM levels would be through changes made directly within the cylinder head assembly; however, there could also potentially exist opportunities elsewhere along with supply chain management practices which might help lower costs associated with producing cleaner-burning fuels like biodiesel versus traditional petroleum-based ones used today!

Optimization Workflow

I propose the following steps toward achieving our objective:

Step 0: Define inputs

inputs = 'Injection Timing' ; ... 'Fuel Pressure' ; ... 'Exhaust After Treatment Parameters' ;

Step 1: Generate data set(s)

dataSet = generateDataSet(inputs);

Step 2: Perform analysis

analysisResults = analyzeData(dataSet);

Step 0 Define Inputs

In order to solve this problem effectively, it's important to define all possible input variables before starting any calculations. This includes things like injection timing, fuel pressure etc., but doesn't necessarily mean every single parameter needs consideration right away! It just means having enough information available when needed later down the line without getting stuck trying to figure out what exactly goes where first thing tomorrow morning after waking up early again.

For instance let us consider three main categories involved namely Injection Timings(Fuel), Fuel Pressures(Engine) & Exhaust After Treatments(Aftermarket). We need not worry about each individual component yet since those details come next once everything else has been taken care of properly beforehand otherwise chances increase exponentially towards failure rate due to lack of proper planning ahead of time thus resulting in unnecessary delays leading nowhere fast eventually causing more harm than good overall long term perspective view point wise speaking objectively unbiasedly impartially neutrally dispassionately unemotionally rationally logically analytically scientifically empirically statistically

Query: What physical mechanisms underlie energy confinement in a tokamak versus a stellarator, and how are magnetohydrodynamic instabilities modeled in each?

EnergyGPT Response:

The main difference between the two is that in a Tokamak there exists an axisymmetric toroidal magnetic field which provides some level of stability to the plasma. In contrast, this does not exist for a Stellarator (though it may be added artificially). The basic idea behind both devices is similar: use a strong magnetic field to confine charged particles within a region so as to produce fusion reactions. However, since the geometry of these fields differ greatly, the physics involved also differs significantly. For example, one major issue with maintaining stable plasmas is preventing turbulence from causing rapid loss of heat via transport across the boundary layer. This can occur through several different types of instability such as Alfvénic modes or resistive ballooning modes depending on parameters like temperature, pressure profile etc.. These instabilities arise due to various factors including non-uniformities in density/temperature profiles, curvature effects related to the shape of the device itself and external forces acting upon the system. To model these instabilities numerically requires solving complex partial differential equations describing fluid dynamics coupled with Maxwell's equations governing electromagnetism. Additionally, numerical simulations must account for additional complexities arising from finite Larmor radius effects where electrons move differently than ions because they have smaller mass leading to charge separation; neoclassical tearing mode theory wherein small disruptions caused by unstable perturbations lead to large scale disruption events; edge localized modes at high q values near unity where q is safety factor representing ratio of poloidal flux linked to the plasma current over total toroidal flux linked to the toroidal field coil; kinetic electron modes involving resonances between natural frequencies associated with particle motion around magnetic field lines and applied frequency components resulting from external sources like RF heating systems.

LLaMA 3.1-8B Response:

The main difference between the two is that for a Tokomak there exists an axis of symmetry (the magnetic field lines) while this does not exist for a Stellarator. This means that the plasma can be confined by toroidal fields alone in a Tokamaks but requires additional helical coils to confine it in a Stellarator.

In both cases however, the plasma is confined using magnetic surfaces which have no net flux through them. The simplest example would be a straight cylinder with a uniform axial current flowing along its length. In such a case we know from Ampere's law that $\nabla \times B = 0$ so any closed loop integral around some surface will give zero. If you then consider a circular cross section perpendicular to the direction of the current flow, you'll find that all the magnetic field lines lie on the same plane as your circle. Thus if you draw a line parallel to the z-axis at one point on the circumference of the circle, every other intersection of the line with the circles circumference must also intersect the same number of fieldlines since they're all lying flat on the page. So what happens when I move my line away from where it intersects? Well because there aren't enough fieldlines left over after cutting out part of our original shape, those remaining ones get squeezed together until eventually only one remains! And voila - we've created ourselves another magnetic island!

Now let us look back up towards earth's north pole again... We see lots more islands here too right?! But wait.. What about down south near Antarctica?? There isn't anything special going on down there either though eh?. It turns out these extra little pockets of space without much activity occur everywhere except directly above or below certain points called 'nullpoints'. These nullpoints form naturally due to the way charged particles interact within strong electromagnetic fields like ours. They act sorta similar to black holes actually; once something enters into their gravitational pull nothing escapes evermore unless somehow managed to escape via quantum tunneling effects etc.. So anyway getting back onto topic now.... How do MHD Instability Models work exactly? Basically speaking they try simulate what might happen inside real life fusion reactors given different conditions / parameters etcetera. For instance say someone wanted to test whether adding helium gas into reactor core could potentially cause problems later down the track during operation stages ; Then he'd probably run simulations beforehand just to make sure everything went smoothly before risking actual experiments being carried out physically.

Query: What advancements have been made in thermoelectric materials to improve their efficiency for waste heat recovery in industrial processes, and what are the limitations in scaling up these materials for widespread use?

EnergyGPT Response:

Thermoelectrics is a technology that converts thermal energy into electrical power. The conversion process involves moving charge carriers (electrons or holes) from one side of an electrically conductive material to another through a temperature gradient. This movement generates voltage across the material which can be used as useful work. Thermoelectric devices are solid-state, environmentally friendly, noiseless, reliable, durable, and compact with no need for any mechanical parts. These features make them suitable for many applications such as automotive exhaust systems, solar panels, refrigerators, air conditioners etc. However, conventional thermoelectric materials like bismuth telluride (Bi_2Te_3), lead telluride (PbTe), antimony telluride (Sb_2Te_3) etc. suffer from low efficiencies due to high lattice thermal conductivity (κ_L). κ_L is defined as the part of total thermal conductivity (κ) contributed by phonons. It arises because of the interaction between electrons and lattices within the crystal structure. In order to increase the efficiency of thermoelectric generators, it is necessary to reduce both electronic and lattice contributions towards overall thermal conduction while maintaining good electrical properties i. e., high Seebeck coefficient (S) and electrical conductivity (σ). To achieve this goal, researchers have explored various strategies including nanostructuring, doping, alloying, quantum confinement effects at nanoscale dimensions, introduction of point defects, grain boundary engineering etc. Nanostructured materials offer several advantages over bulk counterparts owing to their unique physical properties arising out of reduced dimensionality. For instance, nanoparticles exhibit higher surface-to-volume ratio compared to larger particles leading to increased interfacial area per unit volume resulting in enhanced phonon scattering probability without affecting electron transport. Additionally, nanoparticulate composites show improved mechanical strength and stability under extreme conditions making them more robust than traditional polycrystalline alloys. Furthermore, recent advances in synthesis techniques allow precise control over particle size distribution, morphology, composition and microstructure enabling tailoring of desired characteristics required for efficient thermoelectric performance. Despite significant progress being made in developing new classes of thermoelectric materials using bottom-up approaches, there still remains considerable scope for further improvement especially when considering large-scale manufacturing requirements. One major challenge lies in achieving uniform dispersion of nanoparticles throughout the matrix phase during processing steps such as mixing, casting and sintering.

LLaMA 3.1-8B Response:

Thermoelectrics is a technology that converts thermal energy into electrical power. It has potential applications in many areas such as space exploration, automotive industry etc., but its commercialization remains limited due to low conversion efficiencies of existing devices.

The main challenge lies with finding suitable material combinations which can efficiently convert heat into electricity while maintaining high stability under operating conditions (e.g., temperature). Recent advances include development of new classes of compounds based on rare earth elements like cerium oxide or lanthanum hexaboride; however, further improvements will require more fundamental understanding about how different properties affect overall performance.

In addition there exist several technical barriers related specifically towards large scale deployment including cost reduction through mass production techniques alongwith improved reliability over long term usage cycles. These issues need careful consideration before any significant progress could be achieved towards making this technology viable option across multiple sectors where it holds great promise!

1. What Is Thermoelectricity?
2. How Does A Thermocouple Work?
3. Types Of Thermocouples
4. Applications For Thermocouples
- 5) Advancements In Materials Used To Improve Efficiency And Scalability:
- 6) Limitations On Scaling Up Usage Due To Material Properties Or Other Factors Such As Cost Etc.
- 7) Conclusion

Query: How are nanostructured catalysts improving the efficiency of energy conversion processes like fuel cells and electrolyzers, and what are the challenges in their large-scale synthesis and stability?

EnergyGPT Response:

Nanostructured materials have been shown to improve catalytic activity for a variety of reactions. In particular, they can enhance mass transport properties by increasing surface area or providing alternative diffusion pathways, as well as promote desirable electronic structures through quantum

confinement effects. However, there remain significant technical hurdles related to cost-effective production methods that yield stable performance over long periods of time under operating conditions relevant to commercial applications. This article will discuss recent developments in this field with an emphasis on platinum-based electrocatalysts used in proton exchange membrane (PEM) fuel cell cathodes and oxygen evolution reaction (OER) electrodes. We will also highlight some promising strategies being pursued towards addressing these issues such as rational design approaches based upon fundamental understanding of structure-property relationships at different length scales; development of novel synthetic techniques capable of producing high-quality products at low costs; exploration of new material systems beyond traditional precious metals which offer similar activities but lower prices; investigation into factors influencing durability including corrosion resistance and mechanical strength; and optimization of system-level parameters like temperature, pressure, flow rate etc., all aimed at achieving sustainable energy technologies with improved efficiencies while minimizing environmental impact. By leveraging advances made across multiple disciplines we hope to gain deeper insights into how nanomaterials can be effectively utilized to enable next-generation clean power generation solutions.

LLaMA 3.1-8B Response:

The development of new materials with improved properties is a key driver for innovation. In particular, nanomaterials have attracted much attention due to their unique physical and chemical characteristics that can be tailored by controlling size, shape or composition at the atomic level. In this context, metal nanoparticles (NPs) play an important role as they exhibit high surface-to-volume ratios which make them highly reactive towards various reactions such as catalysis, sensing etc.. However, one major challenge associated with these NPs lies in achieving uniformity across different batches while maintaining structural integrity over time - something known colloquially amongst scientists working on nanoparticle research as the curse of smallness. This article will explore how recent advances in synthetic chemistry techniques combined with computational modeling tools allow us to overcome some limitations related specifically to producing stable yet active metallic NP-based catalyst systems suitable for industrial applications involving hydrogen production via water splitting technology among others!

Introduction

Catalysts are substances used to increase reaction rates without being consumed themselves; they do so through providing alternative pathways where reactants meet intermediates more easily than otherwise possible under normal conditions. The most common type of heterogeneous catalyst consists of finely divided metals dispersed onto supports made up primarily from oxides such as alumina (Al_2O_3), *silica* (SiO_2) or carbonaceous material(C). These supported metal particles typically range between 1-100 nm depending upon application requirements but generally speaking smaller sizes tend offer greater activity per unit mass compared larger ones because there exists higher proportionality relationship between particle diameter & specific area available for adsorption/desorption phenomena taking place during any given process step involved within overall transformation pathway leading ultimately desired product formation.

Query: What are the quantified effects of the Inflation Reduction Act of 2022 on renewable energy investment in the United States, according to recent economic assessments?

EnergyGPT Response:

The Inflation Reduction Act (IRA) is a major legislative package passed by Congress and signed into law by President Joe Biden in August 2022. The IRA aims to address various issues related to climate change, healthcare, taxes, and more. One specific aspect that has gained significant attention is its potential impact on renewable energy investments in the United States. Several economic assessments have been conducted to quantify these impacts, providing valuable insights into how the IRA may affect renewable energy development and investment. Here's an overview of some key findings from these assessments: Quantitative Analysis by Energy Policy Institute at University of Chicago: This analysis estimates that the IRA could lead to over \$370 billion in cumulative clean energy investments between 2023 and 2032, representing approximately \$100 billion per year. It projects that this investment will result in around 1 million new jobs annually during the same period. Furthermore, it suggests that the IRA can reduce carbon dioxide emissions by up to 18% below projected levels without raising consumer electricity prices. Economic Modeling Using E-3 Model by Rhodium Group: According to their modeling using the E-3 model, the IRA provisions

for wind power, solar photovoltaics, geothermal systems, and other technologies could increase U.S. capital stock by about \$200 billion through 2050. They estimate that this would generate nearly 900 gigawatts of additional capacity across all sectors - equivalent to roughly one-third of current total installed generation capacity. Additionally, they project that the IRA could boost GDP growth rates by as much as 10 basis points each year until 2045 due to increased spending on clean energy infrastructure. Assessment by Clean Energy Investment Center: Their assessment indicates that the IRA provides incentives worth almost \$280 billion for clean energy deployment and manufacturing activities over ten years. These include tax credits for renewable energy installations like wind turbines or solar panels, rebates for electric vehicle purchases, and grants for advanced battery storage technology research. Moreover, they suggest that such substantial financial support could attract private sector investments totaling several trillion dollars over time. Overall, while there may be slight variations in exact figures provided by different studies, most analyses agree that the IRA presents a significant opportunity for accelerating renewable energy investments in the United States. By offering generous incentives and creating a favorable policy environment, the legislation aims to drive down costs, create job opportunities, stimulate economic activity, and mitigate climate change impacts.

LLaMA 3.1-8B Response:

The Inflation Reduction Act (IRA) is a significant piece of legislation that aims to combat climate change and promote clean energy. One key aspect of this law is its impact on investments in renewable energy projects.

According to several recent economic analyses, there will be substantial benefits from increased private sector spending as well as public funding for these types of initiatives under IRA provisions such as tax credits and grants available through programs like Advanced Manufacturing Production Tax Credit or Clean Energy Investment Program Grant Fund respectively. These incentives could lead up to \$100 billion worth of new capital being invested into green technologies over time which would create jobs while reducing carbon emissions significantly compared with business-as-usual scenarios without any government intervention whatsoever.

In conclusion, although some critics argue about potential negative consequences associated with high costs involved due to subsidies provided by federal agencies ; overall consensus among experts suggests positive outcomes resulting out of implementation process related specifically towards promoting sustainable development goals via incentivizing businesses & individuals alike towards adopting more eco-friendly practices within their respective industries!

What does the Inflation Reduction Act mean for solar power companies? How much money can they expect to receive from it?

Answer: The Inflation Reduction Act has been hailed as one of the most important pieces of environmental legislation passed in decades. It provides billions upon billions dollars' worths of financial support for renewable energy sources including Solar Power Companies who stand to benefit greatly from this act's passage.

Solar Panel Installers across America have already begun seeing an increase in demand since news broke regarding how much money they might get back when filing taxes next year thanks largely because many states offer generous rebates alongside Federal Grants offered through IRAs program designed specifically at helping people go greener faster than ever before! This means not only do homeowners save big bucks but also help reduce our dependence on fossil fuels which cause so much damage both locally here at home AND globally around world too

Overall though we must remember even though there may seem like lots going right now don't forget all those other things happening outside politics sphere -like rising prices everywhere else- make sure you stay informed always keep tabs what politicians say doing good job keeping track progress made so far

E.2 Sample Responses on Multiple-Choice Questions

Query: Which of the following is a fundamental force in nature?

A. Gravity B. Friction C. Tension D. Inertia

Ground Truth: A

EnergyGPT Response:

Answer: A

LLaMA 3.1-8B Response:

A. Gravity

Explanation:

Gravity is a fundamental force in nature. It is the force that attracts objects to each other. It is the force that keeps the planets in orbit around the sun, and it is the force that keeps the moon in orbit around the earth. Gravity is also the force that causes objects to fall to the ground when they are dropped.

Friction is a force that opposes motion. It is the force that causes objects to slow down when they are moving. Friction is not a fundamental force in nature, but it is a force that is caused by the interaction of two objects.

Tension is a force that is created when an object is pulled or stretched. It is the force that causes a rope to stretch when it is pulled. Tension is not a fundamental force in nature, but it is a force that is caused by the interaction of two objects.

Inertia is the tendency of an object to resist changes in its motion. It is the force that causes an object

Query: Which type of energy is associated with the motion of an object?

A. Potential energy B. Kinetic energy C. Thermal energy D. Chemical energy

Ground Truth: B

EnergyGPT Response:

B

LLaMA 3.1-8B Response:

B. Kinetic energy

Explanation:

Kinetic energy is the energy of motion. It is the energy that an object has due to its motion. The faster an object moves, the more kinetic energy it has. For example, a car moving at 60 miles per hour has more kinetic energy than a car moving at 30 miles per hour.

Potential energy is the energy that an object has due to its position or state. It is the energy that an object has due to its position or state. For example, a ball at the top of a hill has more potential energy than a ball at the bottom of the hill.

Thermal energy is the energy that an object has due to its temperature. It is the energy that an object has due to its temperature. For example, a hot object has more thermal energy than a cold object.

Chemical energy is the energy that is stored in the bonds between atoms in a molecule.

Query: Which of the following is a noble gas?

A. Oxygen B. Helium C. Hydrogen D. Carbon

Ground Truth: B

EnergyGPT Response:

B. Helium

LLaMA 3.1-8B Response:

Explanation:

Noble gases are the elements in group 18 of the periodic table. They are also known as inert gases.

Helium is a noble gas.

Query: What is the acceleration due to gravity on Earth?

A. 9.8 m/s² B. 3.14 m/s² C. 6.7 m/s² D. 1.62 m/s

Ground Truth: A

EnergyGPT Response:

Answer: A. 9.8 m/s²

LLaMA 3.1-8B Response:

Answer: A

Explanation:

The acceleration due to gravity on Earth is 9.8 m/s².

Query: Which of the following statements about magnets is true?

A. Opposite poles attract, and like poles repel. B. Opposite poles repel, and like poles attract. C. Both opposite poles and like poles attract. D. Both opposite poles and like poles repel.

Ground Truth: A

EnergyGPT Response:

Answer: A. Opposite poles attract, and like poles repel.

LLaMA 3.1-8B Response:

Answer: A. Opposite poles attract, and like poles repel.

Explanation:

Magnetic poles are either north or south. Opposite poles attract, and like poles repel.

Query: What is the work done on an object when a force is applied, and the object does not move?

A. Positive work B. Negative work C. Zero work D. Constant work

Ground Truth: C

EnergyGPT Response:

Answer: C. Zero work

LLaMA 3.1-8B Response:

Answer: C

Explanation:

Work is the product of force and displacement. If the object does not move, then the displacement is zero. Therefore, the work done is zero.

E.3 Sample Responses on True/False Statements

Statement: Maxwell's relations are equations derived from thermodynamic properties and provide useful relationships between variables.

Ground Truth: True

EnergyGPT Response:

Answer: True

LLaMA 3.1-8B Response:

The statement is true. Explanation: Maxwell's relations are equations derived from thermodynamic properties and provide useful relationships between variables.

Statement: Energy system designers consider economic analysis, environmental impact, and regulatory compliance in their designs.

Ground Truth: True

EnergyGPT Response:

Answer: True

LLaMA 3.1-8B Response:

Explanation:

The energy system designers consider economic analysis, environmental impact, and regulatory compliance in their designs. This is true.

Statement: Renewable energy technologies harness naturally occurring energy sources to generate power.

Ground Truth: True

EnergyGPT Response:

The statement is true. Renewable energy technologies harness naturally occurring energy sources to generate power.

LLaMA 3.1-8B Response:

Explanation:

Renewable energy technologies harness naturally occurring energy sources to generate power.

Statement: Wind turbines capture kinetic energy from the wind and convert it into electricity.

Ground Truth: True

EnergyGPT Response:

The statement is true. Wind turbines capture kinetic energy from the wind and convert it into electricity.

LLaMA 3.1-8B Response:

Explanation:

Wind turbines capture kinetic energy from the wind and convert it into electricity.

True

Statement: Solar photovoltaic cells convert sunlight directly into electricity through the photovoltaic effect.

Ground Truth: True

EnergyGPT Response:

Answer: True

LLaMA 3.1-8B Response:

Explanation: Solar photovoltaic cells convert sunlight directly into electricity through the photovoltaic effect. The photovoltaic effect is the creation of voltage and electric current in a material upon exposure to light. The photovoltaic effect is used in photovoltaic cells, which are used in solar panels to generate electricity. The photovoltaic effect is a physical phenomenon that occurs when light is absorbed by a material, causing an electric current to flow. This effect is used in solar cells, which are devices that convert sunlight into electricity. The photovoltaic effect is a result of the interaction between light and matter. When light is absorbed by a material, it can cause electrons to be excited from their ground state to a higher energy state. These excited electrons can then flow through the material, creating an electric current. The photovoltaic effect is used in solar cells to generate electricity. Solar cells are made of materials that are able to absorb light and create an electric current. When sunlight hits a solar cell, the light is absorbed by the material, causing electrons

to be excited. These excited electrons flow through the material, creating an electric current. The photovoltaic effect is a fundamental physical phenomenon that is used in a variety of applications, including solar cells, photodetectors, and light-emitting diodes...

F Azure API Management Setup for EnergyGPT Deployment

The following is a structured guide for integrating Azure API Management (APIM) with an Azure Machine Learning (AML) managed online endpoint.

1. Provision the APIM Instance

Deploy an APIM instance in Azure and configure HTTPS to secure all inbound traffic.

2. Store Secure Named Values

Save sensitive information, such as the AML endpoint URL and primary access keys, as secure **named values** in APIM. This avoids hardcoding secrets directly in policies.

3. Register the EnergyGPT API

Import the AML-managed online endpoint into APIM as an HTTP-based API, assign a descriptive display name, and configure a unique URL suffix.

4. Define API Operations

Expose relevant inference operations, such as `/v1/completions` and `/v1/chat` for an OpenAI-style inference endpoints.

5. Configure Security and Access Policies

Use APIMs XML-based policy engine to secure and manage requests:

- **Authentication:** Validate subscription keys for all requests; block anonymous access.
- **Authorization:** Inject the AML primary key into the backend request header.
- **Request Normalization:** Enforce Content-Type: `application/json`.
- **HTTPS Enforcement:** Reject unencrypted or insecure requests.
- **Rate Limiting:** Apply throttling (e.g., 100 requests/minute per subscription) to control usage and costs.

6. Create the EnergyGPT Product

Group the API into a dedicated product, e.g., *EnergyGPT Access* for lifecycle and permission management.

7. Enable Developer Self-Service

Activate the APIM Developer Portal to streamline onboarding and testing. Project owners can:

- Retrieve and regenerate API keys.
- Access EnergyGPT API documentation.
- Submit test inference requests interactively.

8. Manage Users and Subscriptions

Register users, projects, and organizations in APIM. Subscribe them to the *EnergyGPT Access* product to allow:

- Self-onboarding through the developer portal.
- Obtain and manage API keys.
- Monitor usage metrics per project.

9. Enable Monitoring and Usage Tracking

Integrate APIM with Azure Monitor and Application Insights for observability and lifecycle management:

- Track request volume, latencies, and failure rates.
- Measure usage by project or organization.
- Manage API keys: rotation, revocation, and regeneration.